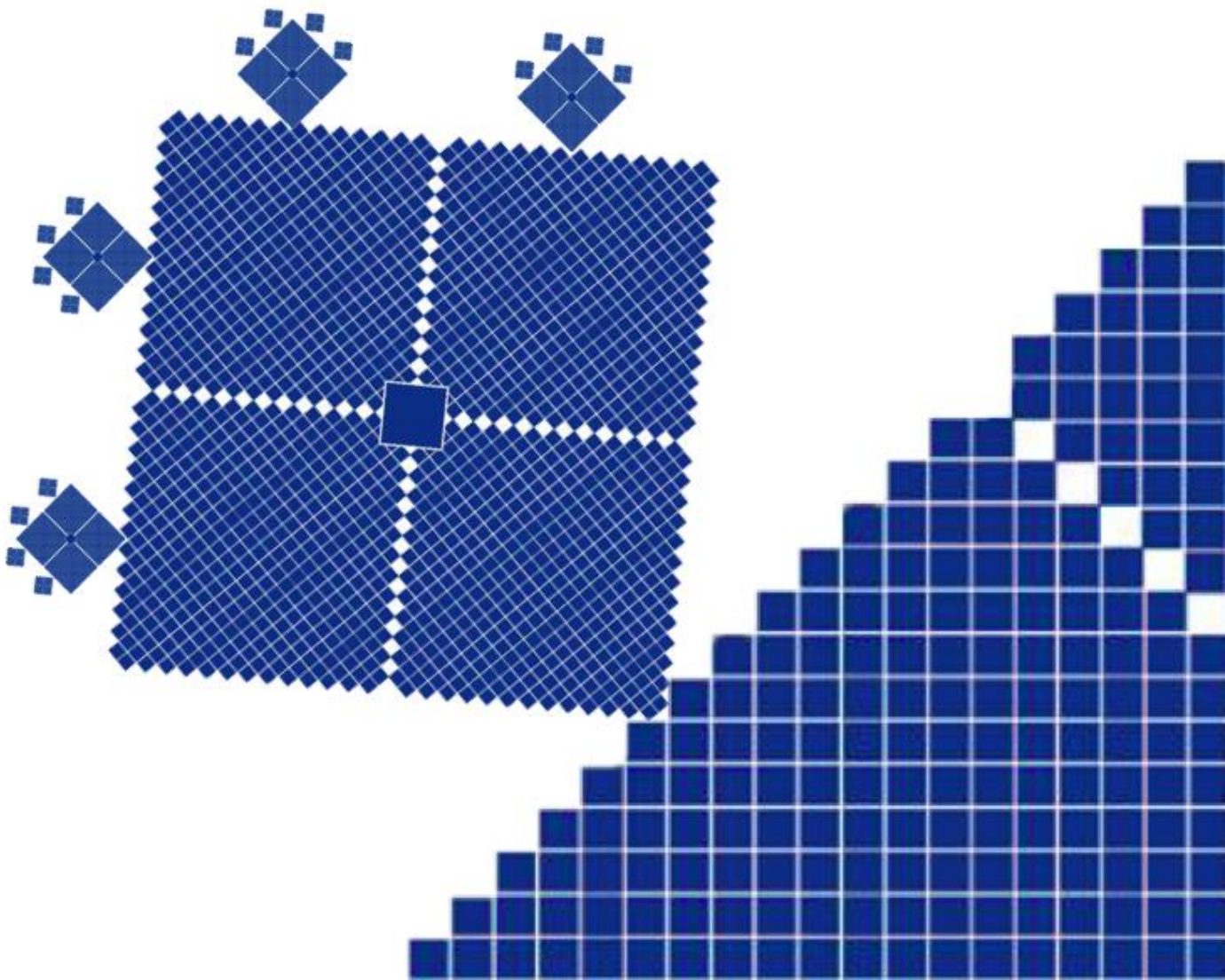# New imaging approach to study the microstructure of amorphous drug formulations based on multifractal geometry

Renata Abreu Villela

New imaging approach to study the microstructure of amorphous drug formulations based on multifractal geometry

Doctoral thesis presented by

Renata Abreu Villela

Supervised by

Prof. Dr. Isidoro Caraballo[1]

Prof. Dr. Martin Kuentz[2]

[1]Department of Pharmacy and Pharmaceutical Technology

Faculty of Pharmacy

Universidad de Sevilla

[2]Institute of Pharma Technology

University of Applied Sciences and Arts Northwestern Switzerland

Sevilla, 2019

Aos meus queridos pais

e à minha irmã.

Cha(lle)nge.

Frank Bodin

Acknowledgements

A PhD thesis is a long journey. The motivation is the dream and the way include many challenges, uncertainty, emotion, euphoric moments, it was necessary to be patience, have energy, think out of the box, leave the comfortable zone and work hard. During this journey many people supported me, directly or indirectly, and I am really grateful.

Mis agradecimientos a Prof. Dr. **I**sidoro Caraballo, mi director de tesis y responsable del grupo de investigación Caracterización y Optimización Estadística de Medicamentos, siempre te estaré agradecida por dejarme ser partícipe de él y la oportunidad de concluir mi tesis doctoral en la Universidad de Sevilla, además de la confianza deposita durante estos años, ¡infinitamente gracias!

I am gratefully acknowledged Prof. Dr. **M**artin Kuentz for giving the chance to spend a great time during my PhD thesis in his group at University of Applied Sciences and Arts Northwestern Switzerland. I appreciated all our fruitful scientific discussion and your valuable inputs for my scientific development. Thanks a lot.

I would like to thank Dr. **M**onika Schönenberger for her expertise and the time spent to analyze my samples. Gracias al CITIUS, en especial a **C**onsuelo Cerrillos González y a **F**rancisco Rodríguez Padial por el conocimiento y la transferencia de informaciones de los equipos.

To my colleges from both group I appreciate you taking time out of your busy day to help me with my projects, it was a pleasure to learn from you. Also, the convivial moment we spend together, especially in Basel, the many lunch breaks, Easter brunch and Christmas dinner.

Live abroad was also about to learn new cultures, and with flat mates from different countries the exchange of culture has been rich for my best self.

It is all about the story or it is better written, it all about the people I met during the journey, and **C**hristoph Stockhamer was the surprise. Thanks to share your experience with

me, the unforgettable moments, the nice words, to trust on me when I could not, my paper publication celebration and the upgrade in my student life style. Danke!

To live in Spain and in Switzerland would not be possible without my language's teachers. Muchas gracias **J**uan Manual Bustamante por todo el tiempo y conocimiento en el descorrer de estos años. Ich bedanke mich bei Herr **S**turm. Deutsch als Fremdsprache zeigt die Facette von einer Kultur, deren Denkart und Verhaltensweise durch ihren Reichtum und Schönheit. Dankschön.

Agradeço a agência de fomento Coordenação de Aperfeiçoamento de Pessoal de Nível Superior (CAPES) que financiou este doutorado.

À minha família que esteva no Brasil, mas em meus pensamentos, aos que vieram me visitar e matar a saudade (tia **R**osana, **K**ika e **D**ea).

À minha irmã **P**aula, ter seu apoio em meus projetos e grandes desafios me ajudaram muito. Os momentos que você estava junto e outros nem tão perto fisicamente e podíamos compartilhar conquistar, dividir frustações, até quando contávamos uma com a outra nos desafios científicos cada uma com seu ponto de vista.

Aos meus pais, **J**orge e **F**átima, que me incentivaram desde o início até o fim na minha aventura no Velho continente. O amor incondicional, a sólida formação dada, os conselhos preciosos, encorajamento nos momentos difíceis, as longas conversas no Facetime, aos mimos quando chegava no Brasil, tão necessários.

Por fim a **D**eus pela energia divina que fez tudo acontecer. Agradeço os momentos marcantes que me transformaram em quem eu sou.

Obrigada! Thanks! Gracias! Danke!

Summary

Chapter 1

General introduction

1.1. Background

Oral dosage forms are the most common pharmaceutical formulations. To be effective and reach their site of action, the drug has to solubilize in gastrointestinal fluids and permeate membranes in the gastrointestinal tract [1][2]. The active pharmaceutical ingredients (APIs) according to Biopharmaceutical Classification System can be classified in class I, II, III and IV, where the class II and IV drugs exhibit low water solubility. The absorption of most of these APIs will be limited by their solubility or their dissolution rate [1][3][4].

The management of these poorly water-soluble drugs is one of the major challenges in the field of pharmaceutics. Many techniques enable to improve the solubility or to increase the surface area available for the dissolution enhancement of poorly water-soluble active pharmaceutical ingredients (APIs) through chemical or physical modifications, for example by using soluble prodrugs and salts, changing the particle size, the crystal lattice (including amorphization and polymorphism), and by using complexes of the drug with adequate ligands. A key strategy used to address solubility issues is the formulation of amorphous dispersions of challenging APIs [3][5][6].

Amorphous solid dispersions (ASDs) are one-phase solid systems that contain an amorphous drug stabilized in one or more polymeric carriers. The amorphous form is a disordered structure with a high free energy. This form presents advantageous

biopharmaceutical characteristics compared to the crystalline form. Targeted is especially , an improvement in the apparent solubility, dissolution rate, and bioperformance for oral delivery [5][7].

The degree of drug dispersion can be reduced to the molecular level in ASDs and the presence of hydrophilic carrier leads to improved wettability of the system and possibly an increase in apparent solubility, due to higher free energy for solubility enhancement based on changes in enthalpy and entropy, as compared with the crystalline form [1][7]. There are three types of ASDs depending on the physical state of the API in the matrix. Thus, a glassy suspension is obtained if the drug is dispersed in an amorphous state and a crystalline suspension is given when the drug remains in the form of fine crystalline particles; finally, a glass solution may obtained if the drug is dispersed at a molecular level [4][8].

The selection of the manufacturing process is very important for the ASD. In general, ASDs are prepared by heat based methods and solvent based methods due their high efficacy, low costs, fewer types of materials involved and a relatively easy way to scale up [3][9]. A possible challenge during the manufacturing process is to avoid the formation of large drug clusters and to prevent any phase separation [9][10][11].

ASDs have proven to be superior to other techniques for oral delivery of poorly soluble drugs, however there is still the concern about thermodynamic instability. ASDs are metastable systems and bear the risk of instability during their shelf life. The manufacture process also influences the physical stability according to thermal history, particle morphology, and nucleation process produced by different methods [10][12].

The molecular processes of phase separation as well as crystallization from amorphous material are complex and mobility in the glass state plays an important role. Relaxation of amorphous materials take place on different time scales, from primary diffusive (α-relaxation) to secondary local relaxation such as Johari-Goldstein relaxations (β-relaxation). While α-relaxation becomes very slow in the glass state, it is mostly the secondary relaxations that are relevant for crystallization from amorphous state [11]–[14]. Once crystallization starts, it continues to reduce the system's free energy [15][16][17]. Thus, thermodynamics is the driver for physical change and molecular mobility is a facilitator, while surface effects can act as modulators, and heterogeneities as amplifiers of crystallization [18].

Despite the general success and advanced knowledge of ASD, as a standard formulation technique for poorly soluble drugs, there are still knowledge gaps, which concern strategies to

accelerate the development and improve performance of ASD [5][14]. Advancement can be expected, for example in the field of analytical characterization and regarding an improved understanding of formulation microstructures. Among the different analytical tools, the image-based methods are particularly becoming relevant nowadays to provide direct insight from phase separation [19] and homogeneity [20][21].

The chemical imaging involves a sophisticated analytical technique for acquisition of images and spectra that contain the chemical information [21], which typically enables to study the spatial distribution of one or all formulation components [22]. Images can be acquired at the surface and in the bulk using different electron microscopy techniques, such as, transmission electron microscopy (TEM) and scanning electron microscopy (SEM) with energy dispersive X-ray spectroscopy (EDS) [17][24][25]. Alternatively the images can also be captured by vibrational spectroscopic techniques with appropriate optics, such as Raman [22][26][27], near infrared (NIR) or terahertz spectroscopy [18].

Depending on the imaging method employed, it can be possible to obtain a clear visual result; nevertheless, it is usually difficult to achieve direct insight just from direct visual assessment of the obtained images. The image displays generally a complex cluster structure that is difficult to compare and to interpret at a specific length scale. Therefore, there is often a need of data processing once images are obtained in order to extract relevant structural data from solid dosage forms. However, it can be even more attractive to apply a mathematical model for characterization of heterogeneous physical structures such as fractals.

Fractal is a concept of non-classical geometry proposed by Mandelbrot [27] to describe spatially and temporally, objects, systems, and phenomena [28]. Fractal dimensions provide here information about the irregularities of the system. In general, a high difference between the Euclidean dimension and the fractal dimension indicates a high level of irregularities of the studied system [29]. An essential concept of fractal theory is self-similarity, where the random chaotic irregularities present in a heterogeneous complex have often a type of fractal order across scales. This self-similarity is possible to be expressed mathematically as the range of magnification where the structure of a system keeps a similar pattern and therefore a constant fractal dimension [30]–[32].

Since fractals are ubiquitous in nature, the concept of fractals has been used in various scientific fields, including pharmaceutical sciences in which many different types of disordered or disordered systems or chaotic systems can be described by the theory. Applying the concept

of fractal time series analysis bring benefits to the management of chaotic and random systems, developing an atomic level understanding of different solid systems [33]–[36].

To experimentally determine fractal dimensions, different techniques can be used. The best known box-counting method was developed for this purpose and can be used to quantify simultaneously porous channels and surface structures [37]. For solid pharmaceutical dosage forms, the irregularity degree of a subject can be highly abstracted into a non-integer fractal dimensional value (Df). The Df values may describe objects in a three-dimensional Euclidean space such as solids or porous structures but also surfaces can be studied. Thus, particle geometry can be assessed as well as surface roughness, particles shape, and size and the degree of spatial complexity [32][37].

Fractal geometry provides insights into the microstructure formed during a manufacturing process that cannot be otherwise obtained by conventional analytical approaches [30][37]. Interesting is in particular , the multifractal spectrum that can be used to provide information on the subtle geometrical properties of a fractal object, which cannot be otherwise fully described by a single fractal dimension [36][38]. The formalisms of multifractals express a generalized fractal dimension (Dq) and a moment order (q) that is a number within [$-\infty$; $+\infty$] interval extracting characteristics of the cluster distribution [39]. The multifractal spectra or the generalized dimension can be restricted to three values of particular interest D_0, D_1 and D_2. Herein, D_0 is the "classical box-counting dimension" also called the "capacity" dimension; D_1 refers to an information dimension (related to Shannon's measure of entropy) and characterizes the degree of disorder in a distribution. Finally, D_2 is named "correlation" dimension so it indirectly marks a degree of clustering [39]–[43]. In the case of monofractal systems, $D_0 = D_1 = D_2$, whereas on the other hand, different values $D_0 \geq D_1 \geq D_2$ indicate a multifractal system [39].

1.2. Motivation and objectives

As it has been explained in the previous section, despite the success of ASDs, there is a need for improved tools able to provide a better understanding of these complex disordered systems and that should help predicting the stability behavior of ASDs. The application of these tools would enable a more efficient and faster development process, while ensuring a high-quality of ASDs.

Hence, the general objective of this PhD thesis is to develop a coupled image based analytical tool linked to fractal approach, to enable study of the microstructure and to improve the process understanding of solid pharmaceutical formulations containing amorphous APIs. This thesis is divided into individual chapters which introduce the approach for microstructural characterization of these complex formulations.

A first specific objective of this thesis is to introduce the fractal analysis for evaluation of drug distribution in ASDs by considering the approach of multifractal geometry. There is a specific aim to evaluate the impact of the addition of urea on the ASDs microstructure, once this excipient has shown promise for reducing the manufacture temperature as well as to improve drug release.

Given that physical stability is a major concern about amorphous materials, since the amorphous drug in ASDs is prone to revert to its crystalline form. A second objective of the present thesis was to evaluate if the fractal analysis based on energy dispersive X-ray imaging can provide the means to identify early signs of physical instability from ASDs, which are typically not detected by standard methods like X-ray powder diffraction.

Finally, another aim of the present work was to apply the multifractal data analysis for assessing the impact of different manufacturing techniques on the microstructure and performance of the obtained ASDs.

Chapter 2

General results and discussion

This chapter summarizes the general results and discussion of the microstructural study via fractal geometry based on chemical imaging to gain insights concerning properties and performance of ASDs.

It is evident from the literature that SEM-EDS is a most commonly used technique for representation of elemental composition from micro-scale surfaces, with a detection limit of approximately 0.1% [44]. Since SEM-EDS application focusses on elemental specific localization and distribution on the compact surface, model drugs that contain Cl atoms were selected. Such halogen atoms are generally well detected by SEM-EDS given that their elevated atomic number facilitates relatively higher X-ray scattering intensity in organic molecules. Specificity of the analytical method was given because the Cl atoms were only present in the drug molecules but not in any of the excipients used.

The images obtained from SEM-EDS by the naked eye can barely provide insights beyond the finding of an absent larger-scale phase separation. For a more refined cluster analysis, this work introduced the multifractal approach.

2.1. Multifractal analysis for drug distribution in ASDs

The multifractal analysis was employed as a tool to quantify the complexity and spatial heterogeneity of compounds in ASDs. As previously mentioned, the drug can be incorporated differently in a matrix dependent on the type of the amorphous formulation. Drug clusters can exhibit very different space coverage and the degree of disorder and level of clustering can show differences.

ASDs were prepared using HPMCAS-LF and different drugs: amlodipine (AML), felodipine (FEL), glybenclamide (GLY), and indomethacine (IND). The multifractal analysis showed that the evolution of Dq versus q for the formulations AML10 (Amlodipine 10% w/w), FEL10, GLY10, and IND10 displayed sigma-shape where Dq decreased with higher values of q. This showed that the multifractal approach did not introduce any unnecessary complication because a simpler monofractal model would be clearly inadequate, as it would assume a single constant fractal dimension along different values of q.

It was interesting to investigate the specific influences of given compounds on the multifractal dimensions. The results showed that the obtained fractal dimensions were influenced by drug loading: rising drug concentrations increased the different dimensions indicating a higher space coverage (D$_0$), higher dimension of disorder (D$_1$), and higher correlation dimension (D$_2$), which in turn suggested a lower degree of clustering.

The observed effect of compound was also statistically analyzed at a reference drug load of 10% (w/w). The API effect in D$_0$ showed a pronounced difference between AML-FEL and FEL-IND. An interpretation of this result was that molecular interactions of the compound with HPMC-AS would define a particular microstructure of how drug clusters form in an ASDs. For D$_1$ and D$_2$ APIs were obviously affecting in their particular way the microstructure of the SDs even though the trends in changes of fractal dimensions were quite comparable. Any simpler assumption of a homogenous drug distribution in SDs or a distribution that can be described as a monofractal system would fall short in light of the results obtained.

To extend the multifractal approach to more complex systems, ternary mixtures with a concentration of 5% w/w urea were analyzed. For chemical imaging, this approach resulted in "pseudo-binary images". The multifractal analysis of API distribution indicated a lower generalized dimension on formulation with urea, corresponding to a lower space coverage (D$_0$), lower heterogeneity (D$_1$), and higher clustering level (D$_2$). In contrast to all other APIs, ASDs of IND and polymer had lower values of D$_0$, D$_1$ and D$_2$ than IND formulations with added urea. From a mechanistic perspective, urea could have different effects. Owing to its particular structure, urea has the ability to interfere with hydrogen bonding. An influence of urea on hydrogen bonding patterns in solid dispersions is therefore interesting but would require additional spectroscopic studies for clarification. There could be also general effects of urea on the cluster structure so that a simple dilution of polymer could have played a role in the observed fractal dimensions of the ternary mixtures.

2.2. Multifractal approach in the early stages of physical instability

The metastable character of ASD is a hurdle for their development because of re-crystallization. It is particularly critical when such physical instability is only detected late in pharmaceutical development, whereas an early identification of kinetically unstable formulations is less problematic in a screening phase. Accordingly, there is a tremendous interest in early identification of drug phase separation and re-crystallization from amorphous state. Based on the hypothesis that multifractals can be helpful to early detect instability in amorphous drug formulations, a stability study was performed, focusing on the early stage of stability testing, which did not reveal re-crystallization based on classical XRPD testing.

The different D_q values were pointing to multifractals as a better model than a simpler monofractal cluster distribution. A typical sigmoidal shape was evidenced with decreasing D_q along decreasing q values.

Since the multifractal dimensions provide meaning to cluster distributions, they can prove helpful for understanding any early changes in ASD, but the physical interpretation of these clusters should be always in the context of the applied imaging method. The dimension D_0 describes a space-filling capacity and values decreased in the early period of stability testing. This result was not easy to predict because there are different possible processes like drug migration to the surface that may increase the space-filling capacity. An increase could also come from drug that was previously too dispersed and low concentrated to be detected as a drug-rich domain so that local aggregation can lead to new clusters. While these are processes to increase D_0, there are other effects that may potentially lead to lowered values of this capacity dimension. Some of the drug-rich domains of drug-polymer aggregates may locally become more concentrated in an overall phase separation or drug re-crystallization. The resulting more concentrated clusters would appear still white in the binary images so that overall space coverage could slightly diminish.

The different cluster changes were apparently also leading on the average to a reduction in the information dimension D_1. This dimension reflects the diversity of elements in the system. Moreover, D_2 holds for a correlation dimension and the evidenced reduction was caused by the microstructural changes. Thinking of the transformation from amorphous

clusters to crystals there is of course nucleation as well as growth. Depending on which mechanism prevails, there would be different ways of how the correlation dimension changes. Regarding microstructural processes of phase separation, or crystal nucleation and growth, it is possible that different processes affect fractal dimensions in opposite directions, which could entail a loss of discrimination. The sensitivity to detect early physical instability by the multifractal approach is therefore certainly depending on the physical processes that occur as well as on the imaging technique used.

The selected model systems showed some physical changes after four weeks with likely initial phase separation and occurrence of first crystals at the time of four weeks. Differences in the multifractal dimensions D_0, D_1, or D_2 were indeed evidenced after one month compared to the initial analysis. Therefore, multifractals were capable of revealing microstructural changes caused by instability that were otherwise hard to identify from the original images of SEM-EDS and that were undetected by X-ray powder diffractograms (XRPD). It was in line with expectation that laser scanning confocal microscopy (LSM) and atomic force microscopy (AFM) were more sensitive methods than XRPD to capture changes so these reference methods were interesting to compare with the novel multifractal approach based on SEM-EDS imaging.

2.2. Multifractal approach and influence of manufacturing technology

ASDs can be processed by solvent based methods, heat-based methods, mechanochemical activation or a combination of these. The solvent based and heat based are the most commonly applied techniques. The first ones include techniques such as spray drying, solvent controlled precipitation, fluid bed, and supercritical fluid based technologies; the second kind of methods involve techniques as melt extrusion, melt granulation, and ultrasonic assisted compaction [45][46]. Depending on the selected manufacturing technique, an ASDs could have different behavior. For example, the type of interactions that may occur in solvent based methods can be different from that of heat-based methods, resulting in different microstructure and hence product performance.

The XRPD analytical technique showed that all methods of preparation employed resulted in amorphous material, but XRPD did not provide further information about the amorphous phase. Thus, any presence of amorphous-amorphous phase separation should be

avoided as it can lead to drug crystallization. The analysis of differential scanning calorimetry (DSC) showed the presence of a single T_g indicating a homogeneous mixing, but it is known that a limitation of this method is detection of about < 30nm clusters to detect microstructural phase separation [47]. Complementary techniques are therefore needed to investigate such phase changes and imaging-based techniques provide here promising analytical options. The chemical imaging techniques are advantageous to detect clusters formation, even though the spatial resolution limits impact on the cluster's determination. The clusters, which describe drug-rich regions of different types (as separate amorphous domains or small crystals) can be seen as mathematical objects with their characteristic fractal dimensions. Thus, fractal geometry could possibly be applied as a model of microstructural differences to obtain guidance on the selection of pharmaceutical manufacturing processes.

The differences in the multifractal dimensions D_0, D_1, and D_2 evidenced the differences in the microstructures that resulted from the selected manufacturing techniques. Such rather subtle differences would be otherwise hard to identify or even quantify from the original images of SEM-EDS. Table 1 shows the results of multifractal analysis in terms of the dimension with q values from zero to two. The difference between the values of Dq, that decrease with increasing q values, evidenced that the multifractals was a better model than the simpler monofractal cluster distribution, which would entail a constant Dq.

Table 1

Generalized fractal dimensions based on chemical imaging and conversion to binary pictures of indomethacine (IND) solid dispersions obtained with different manufacturing techniques.

	Method	Generalized fractal dimensions		
		$D0$	$D1$	$D2$
IND/HPMCAS-LF	Solvent coprecipitation	1.86 ± 0.02	1.84 ± 0.01	1.79 ± 0.01
(15:85)	Solvent drying	1.75 ± 0.02	1.73 ± 0.02	1.68 ± 0.02
	Melting	1.78 ± 0.01	1.77 ± 0.01	1.72 ± 0.02
IND/HPMCAS-HF	Solvent coprecipitation	1.84 ± 0.01	1.82 ± 0.01	1.77 ± 0.01
(15:85)	Solvent drying	1.75 ± 0.00	1.73 ± 0.00	1.70 ± 0.07
	Melting	1.75 ± 0.01	1.74 ± 0.01	1.69 ± 0.02

The dimension D_0 describes the space-filling. High values can be indicative of drug migration to the surface that may increase the space-filling capacity, whereas lower values could be due to some concentrated clusters of drug-rich domains of drug-polymer aggregates

in an overall phase separation during the manufacturing process. The information dimension (D_1) refers to the diversity of elements in the system, lower values suggest concentration of particles in a small domain. Finally, smaller values of D_2 (correlation dimension) could indicate that the isolated clusters are prevailing versus the pore clusters, this could indicate initial amorphous-amorphous phase separation with drug-rich clusters that can cause future instabilities of amorphous systems.

All D_q values were analyzed statistically. An analysis of variance (ANOVA) was conducted showing that the generalized fractal dimensions (D_0, D_1, and D_2) were indeed statistically significant ($p < 0.0001$) to capture the microstructure variations regarding the different manufacturing techniques (see Fig. 1). The grade of HPMCAS was also significantly influencing D_0, D_1, and D_2. A significant p value was also evidenced for the interaction between the method of ASDs production and the HPMCAS grade show. Fig. 1 shows a statistical means plot together with Tukey's 95% HSD intervals. The significant of the technique applied was similar for all fractal dimensions. In figure 1 is shown for D_0.
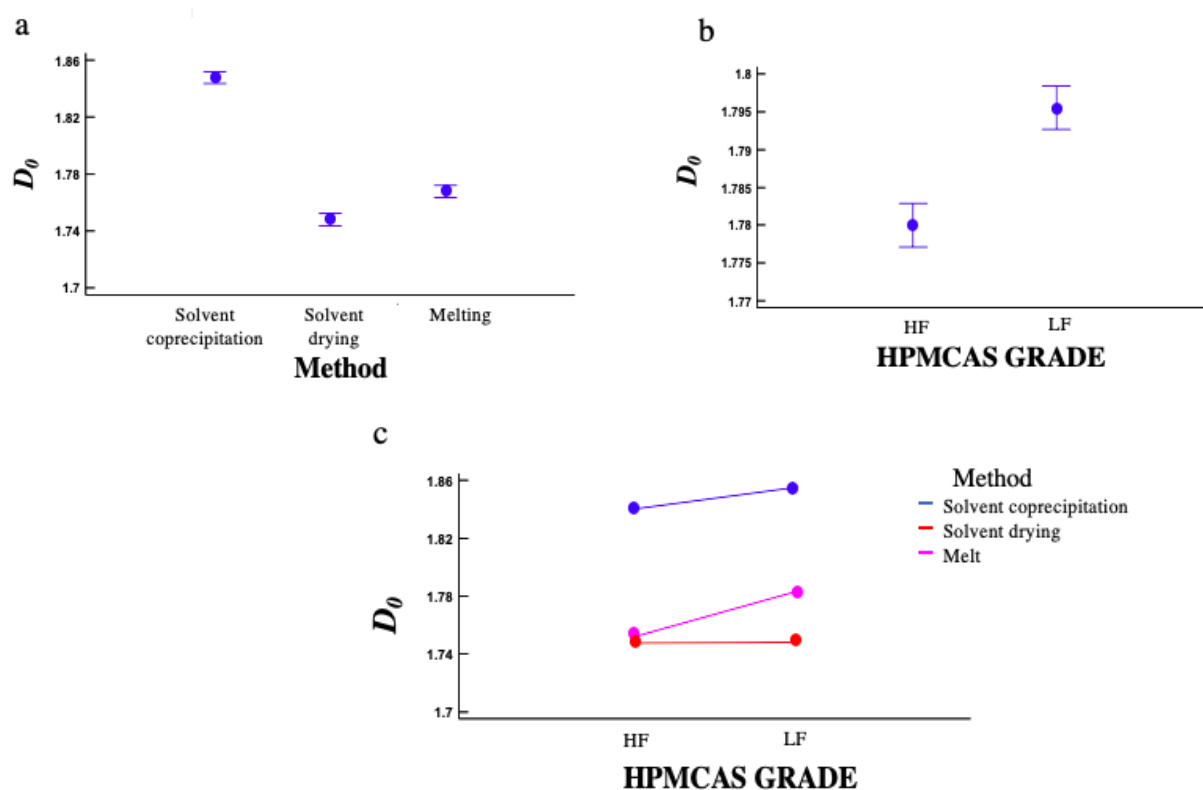

Fig. 1. Statistical means plot of analysis of variance from IND/HPMCAS ASD formulation (15% wt% of IND) based on sums of squares ANOVA how D_0 is affected by the manufacturing technique(a); the HPMCAS grade impact (b) and the interaction plot between the technique applied and the HPMCAS grade (c), the intervals of Tukey's honestly significant difference (HSD, 95%) are shown.

The values obtained for the capacity dimension D_0 were clearly below the Euclidian dimension ($D=2$) but still relatively high for all the manufacturing techniques. The D_0 values for the solvent coprecipitation method for both polymer grades were considerably higher compared to the others, indicating that a more complex and irregular surface was obtained with this technique. This could be attributed to small crystals whose presence, was confirmed by the LSM analysis. The presence of crystals could be due to an incomplete conversion of the drug into the amorphous form. The values obtained for melt and solvent drying methods were similar, for the HPMCAS-HF the values were the same. With respect to D_1, the values for solvent coprecipitation method were also appreciably higher compared to the other techniques. The melt and solvent evaporation techniques for HPMCAS-LF show a considerable difference being significantly higher for the melt method. On the other hand, for the HPMCAS-HF formulation the values were practically similar. Comparing the values of D_2, the solvent evaporation method had rather small values. This could be due to the molecular mobility and the subsequent molecular re-orientation following solvent evaporation.

Thinking of the microstructure and the manufacturing technique, the solvent evaporation method consists of an initial solubilization of drug and polymer in a common solvent (or a mixture of solvents) followed by solvent removal. This can give rise to the formation of non-covalent molecular interactions that are mainly responsible for the amorphization of drug. During the solvent coprecipitation technique, the use of organic solvents and antisolvent (water) represents already a medium with a comparatively high dielectric constant that can facilitate charge separation. Another difference to a classical solvent step such as spray drying is that the removal of solvent is comparatively slower. Such differences enable the formation of different molecular interactions, such as ionic, H bonding, dipole-dipole and van der Waals interactions. By contrast to any solvent-based method, the melting method is achieved by heating that enables a certain molecular mobility and a subsequent molecular re-orientation and formation of drug-polymer interactions. In our study, increased temperatures were obtained by the ultrasonic energy applied during the compaction that provided heat and pressure.

Regarding to the HPMCAS grade, the LF grade showed higher values for D_0, D_1, and D_2 compared to the HF grade, which was attributed to a different substitution pattern between the grades. The HF grade has a relatively higher percentage of acetyl over succinoyl substitutions, which is opposite to the substitution pattern in the LF polymer grade.

The likely differences in molecular led to a decrease in the value of D_0, D_1, and D_2. In relation to the technique selected, this is true for solvent coprecipitation and fusion method, while no substantial decrease was observed for solvent evaporation.

From these results, it can be stated that the given melting method was the most promising manufacturing technique for this studied system, IND-HPMCAS, based on the values obtained for multifractal approach and the implications these values may have on the microstructure, we can assume that for this combination the energy input was relevant for amorphization. Moreover, the solvent evaporation with the drug rich domains could induce future instability while the solvent coprecipitation even resulted in an incomplete amorphization. Therefore, a preferential order of techniques for this system is as follows: melting > solvent evaporation > solvent coprecipitation.   Regarding to the HPMCAS grade, the HF was deemed as the best grade for melting and solvent coprecipitation method.

Chapter 3

Benefits of fractal approaches in solid dosage forms development

Summary

Pharmaceutical formulations are complex systems consisting of active pharmaceutical ingredient(s) and a number of excipients selected to provide the intended performance of the product. The understanding of material's properties and technological processes is a requirement for building quality into pharmaceutical products. Such understanding is gained mostly from empirical correlations of material and process factors with product's quality attributes. However, it seems also important to gain knowledge based on mechanistic considerations. Promising is here to study morphological and/or topological characteristics of particles and their aggregates. These geometric aspects must be taken into account to better understand how product attributes emerge from raw materials. Regulatory agencies worldwide are promoting innovative strategies that intend to create models based on scientific knowledge, such as physical or mathematical models, in order to design quality into a final product. This review deals with pharmaceutical applications of physical and mathematical models, focusing on percolation theory, fractal, and multifractal geometry. The use of these approaches improves

---

the understanding of different aspects in the development of solid dosage forms, for example, identifying critical drug and excipient concentrations. The aim is to link microstructure with macrostructure of pharmaceutical solid dosage forms as a strategy to enhance mechanistic understanding and to facilitate their development and manufacturing processes.

3.1. Background

The pharmaceutical industry constantly designs and develops new drug products, and improves their product development processes, with solid dosage forms as a preferred option, at least for small molecular drugs. The development from initial formulation design up to the final form and its translation to the market involves substantial labor time, cost, energy, and raw materials consumption [21][48]. Any reduction of the resource investment based on novel modelling approaches is expected to have a high industrial impact.

The adequate selection of components and technology for the development of a formulation is required to meet high product quality expectations [21]. The quality is assured by understanding and controlling the relationship between formulation (drug and excipients attributes) and manufacturing variables (process parameters) [49]. These factors have a direct impact on the evolving microstructure [50], properties, and potential applications [21] of the dosage form.

A range of imaging techniques such as scanning electron microscopy, transmission electron microscopy, profilometry, atomic force microscopy, Raman and near-infrared imaging are currently available to study outer surfaces and cross sections of solid particulate systems. The topography represents the microstructure of a sample, with a given spatial resolution and thereby provides a complex data set [51]–[53]. The data of surface topology can be complex as displayed in Fig. 2, which shows examples of uncoated tablets that were obtained by optical profilometry. Such data can be combined with chemical imaging so that spatial information is linked to the entire spectra. When imaging is two or three dimensional, large datasets are generated that can be substantially difficult to manage and interpret.
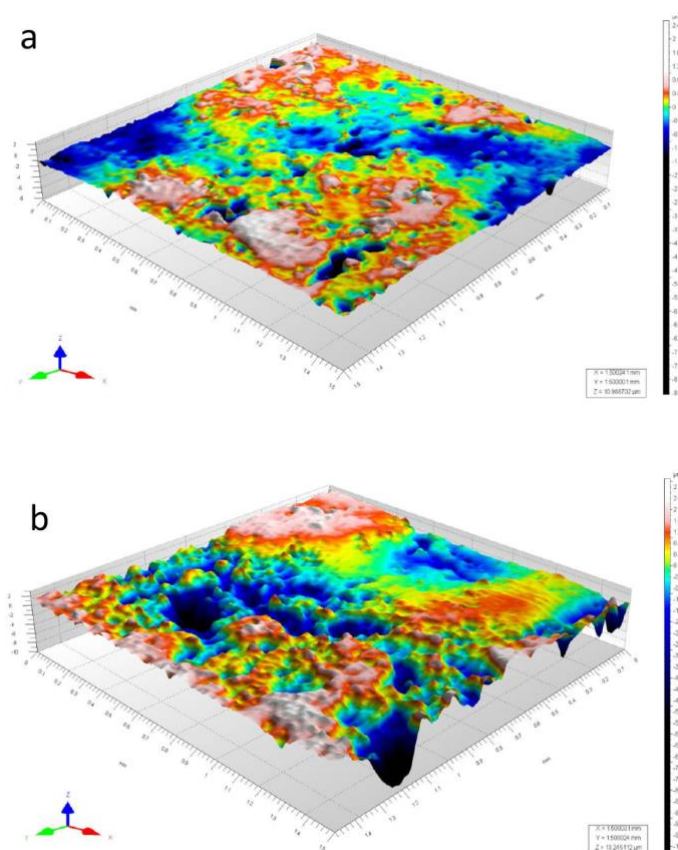
Fig. 2. Example of optical profilometry of uncoated tablets with (a) comparatively lower surface roughness and (b) tablet core exhibiting a rougher surface topology. Details are given in the text.

Models are needed to capture structural features and to generate correlations with relevant properties. Thus, the use of statistical tools helps to understand the relationship between the microstructure and the properties of the drug product in a science-based approach [54].

Descriptive mathematical model platforms can be used for interpretation of the results during the manufacturing process to predict the system properties but also for designing new robust formulations with suitable quality [48][55][56].

This review focuses on fractal modelling approaches. It also describes the use of percolation theory to identify the critical points (e.g. drug or excipient concentrations) related to geometrical phase transitions of the system components, as a tool to define the design space. Moreover, further applications of fractal and multifractal approaches in pharmaceutical development of solid dosage forms are outlined. These tools provide an attractive and

alternative path to gain insights into the characteristics of a formulation and could help with defining robust processes as needed by the pharmaceutical industry.

3.2. Quality by Design (QbD)

In the pharmaceutical industry, the companies are committed to improving the process control and product understanding. Quality by Design (QbD) was proposed by the Food and Drug Administration (FDA) and International Conference on Harmonization (ICH) as a systematic and innovate approach based on quality construction through the understanding of the relationship between the experimental factors and their impact on the quality attributes with minimum experimental runs offering a maximum return in terms of information [57]–[59].

The QbD approach improves confidence in quality throughout the lifecycle of pharmaceutical products development and manufacturing, using risk management, and science-based manufacture principles. [49][59]. Several QbD tools such as product design, process design space, control space, operating space, and process analytical tools are frequently embedded in a risk-based approach [49].

During the development and regarding the manufacturing process, an appropriate control strategy should be developed. The study of parameters that impact the critical quality attributes provides the design space that together with an established control strategy are indispensable elements of contemporary product design and process development [59].

A central position in the arsenal of QbD tools is taken by diverse analytical and process analytical methods, which have the potential to identify relevant properties as well as errors and deviations during the process to guaranty the quality of the products. Process analytics introduces a time domain to already complex data sets obtained from, for example, spectroscopic imaging. This underpins the aforementioned need for suitable mathematical or statistical modelling to cope with the flood of acquired data [60][61].

3.2.1 Design Space

The design space is part of a control strategy, a combination and interaction of material's attributes and/or process parameters that provides assurance of quality. Critical material attributes and process parameters are linked to critical quality attributes either by

statistical or mechanistic models. The material's attributes and the manufacturing operating variables are defined in an acceptable range, including a quality assurance risk probability, and at the end, the product should provide similar quality specifications [49][58][62].

The design space is based on the understanding of the product behavior and reduces the need for a larger amount of data [59]. To gain such understanding within restricted factor ranges, there are QbD tools, for example, design of experiment (DoE) that make use of linear to non-linear models [63]. The latter non-linear models are usually polynomials of second degree. However, at a critical point (i.e. critical concentrations of drug/excipient) there are highly non-linear effects that generally call for a more mechanistic modeling of the data and such a modeling tool is given by the theory of percolation. This approach has proven utility in the estimation of critical points of a formulation to predict the design space [56][64].

3.2.2 Percolation Theory

In order to design a formulation with desired properties, it is crucial to know the basic properties and the spatial distribution of the employed substances. The components of a particulate systems (i.e. pellets, tablets) are expected to be randomly and often not homogenously distributed, which makes prediction of any mechanical properties difficult. If the degree of disorder is low, the behavior of the system can be predicted using renormalization tools; the opposite occurs if the medium is close to a percolation point, where disorder becomes very relevant [65]. Currently, percolation is a highly vivid and fascinating area of modern research that is reflecting many aspects of critical phenomena in an elegant way [66][67].

Percolation theory is a statistical physics approach able to describe a random distribution of disordered systems, based on their spatial correlations. It provides a framework to characterize geometrically how clusters of a components exhibit scale invariance, which can be also seen in experimental imaging[67]–[69]. Percolation is essentially a geometric approach to describe a geometric phase transition and it can be applied to model experimental parameters in the vicinity of a critical point, i.e. a percolation threshold.

Percolation theory simultaneously describes a system's cluster distribution and models' critical properties to achieve physical insights. Percolation is grounded on a rigorous mathematical basis and has a very robust nature and stability in dealing with complex and dynamic models against small perturbations [34][67][68][70]. Despite its rather simple rules,

percolation theory has successfully been applied to describe a large variety of systems in natural, technical, and even social sciences [67].

The origins of percolation theory go back to Broadbent and Hamersley who proposed the basic concept and popularized the theory [67][71]. From a mathematical perspective, the concept of percolation is interesting due to the existence of a critical probability; on either side of the critical probability, the system behaves in different ways. One can imagine a lattice where sites are either occupied with a certain probability p or they are empty with the probability 1- p (i.e. site percolation). Instead of occupied sites, one can also think of setting bonds in a lattice with probability p (i.e. bond percolation). With increasing p, neighboring occupied sites (or bonds, respectively) form clusters that grow in size. A well-defined percolation threshold exists for which a sample- spanning cluster is formed for the first time. This incipient cluster exhibits a fractal nature [72].

A physical correlation could exist on an atomic scale or it can be, for example on a scale of a porous particulate system where percolation occurs as connecting transport and diffusion once a percolation threshold of pores has been reached [34][73]. In pharmaceutical solid systems, a percolation threshold can be assigned to the minimum concentration of a given component at which it is expected to appear as sample- spanning cluster (or "infinite cluster" in the mathematical model) of this specific component, this means that above its critical mass volume (or mass) fraction, one component dominates the properties of the mixture [56][69][74]. In order to find this concentration, it is essential to have experimental systems (i.e. tablets, pellets, granulates, solid dispersions, extrudates, microspheres, etc.) with similar structures (i.e. porosity) but different component ratios [69][75]. Once a component reaches its percolation threshold (p_c), the system undergoes a geometrical phase transition and this percolating component starts to extend over the whole system (Fig. 3). This influences the properties of the system in a non-linear way and it is possible to model different physical properties by power laws in the proximity of the percolation threshold, which is also called a critical point [56][67][71].
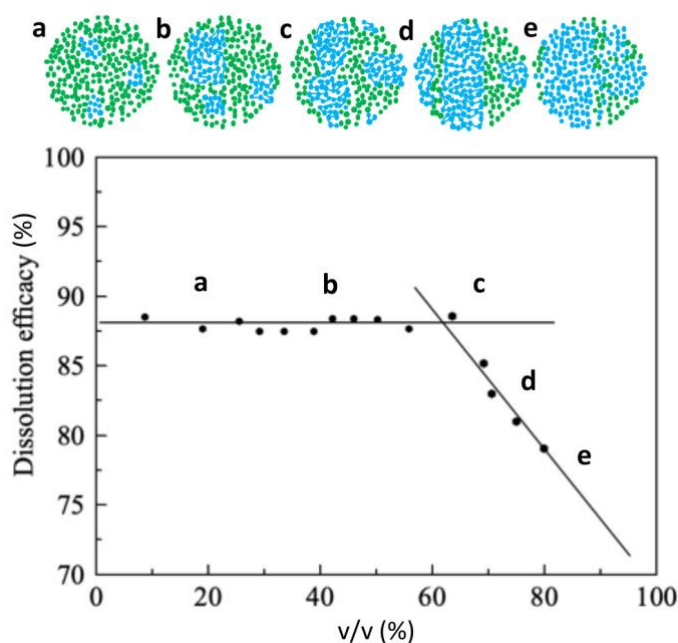
Fig. 3. Representation of a binary system where the dissolution efficacy is plotted against the fraction (% v/v) of A (blue) and B (green) particles, with an increasing concentration of A towards the percolation threshold (critical concentration). The five points (a-e) in the graph and the related snapshots of the system correspond to 2D representations of the microstructure. The point (a) show isolated A particles; point (b) exhibits the initial clusters formation of A particles; point (c) correspond to the percolation threshold of the A particles with a cluster from bottom to top and; (d) and (e) refer to systems where the component A is above its percolation threshold. Details are given in the text.

The so-called correlation length characterizes the structure of the clusters below and above the percolation threshold [34][70]. The nature is only revealed on length scales smaller than the correlation length diverges in the percolation model to infinity at p_c. Applied to physical systems this means that above the percolation threshold, a sample exhibits disorder throughout the entire sample. Thinking of pharmaceutical dosage forms, it is between the percolation thresholds of drug and excipient that both components form interpenetrating percolating clusters [74].

A physical (i.e. experimental) percolation threshold depends on the details of the system, such as drug solubility and particle size [76][77]. Below its percolation threshold, the clusters of the given component are finite and isolated. The percolation theory explains the evolution of the mechanical properties of compacts and mechanisms of tablet formation. This involves a volumetric ratio of components and is linked to external properties, i.e. tensile strength [54], water uptake [78], disintegration time [79] and intrinsic dissolution rate of tablets [75][80].

Apart from the aforementioned transport properties such as drug release from porous compacts, percolation theory has been also used to model mechanical properties of tablets as elastic modulus [81], compression behavior [82], and tensile strength [83][84]. Most of these experimental studies found rather broad ranges in which power laws of percolation theory were successfully applied.

3. 3 Microstructure dynamics in a geometric view

The formation and growth of clusters from individual particles or components is of high interest in complex heterogeneous systems [85]. The microstructural evaluation provides significant insight into the formulation performance. Controlling the microstructure of a pharmaceutical formulation is a key challenge and detailed features of the microstructure are even rarely known in formulation development. Accordingly, there is only an indirect control via the quality attributes of the final dosage form. It is known that the surface of many heterogeneous complex systems shows geometric irregularities together with defects. They are often self-similar upon variation in resolution. Such self-similarity characterizes a mathematical fractal. Unlike mathematical fractals, physical structures generally exhibit a fractal nature only in limited spatial or temporal ranges [27][86].

Fractal is a geometric notion proposed by Mandelbrot and was further depth theorized by Evertsz and Mandelbrot [39] to describe in a fractal dimension (which is a non-integer number) the spatial and temporal self-similarity of objects, systems, and phenomena, based on an extension of the conventional Euclidean geometry [35][39]. Since fractals are ubiquitous in nature, the concept of fractals has been used in various scientific fields, including pharmaceutical sciences, to evaluate the geometry of a sample and mapping a structure in diverse quality parameters and to monitor chaotic systems performance (i.e. by time series analysis) [33]–[36].

Fractal geometry provides an understanding of the formation of the microstructure during the manufacturing process [30][87] that is hardly obtained by other conventional methods [88]. For solid pharmaceutical dosage forms, self-similarity and hence the irregularity degree of an object or feature can be represented by a non-integer fractal dimensional value (Df). The Df values can be derived, for example, from surface imaging techniques to characterize the geometry, surface roughness, particles shape, or size as well as the degree of

spatial complexity [32]. Smooth surfaces, for example have a low fractal dimension, whereas highly textured surfaces have a high fractal dimension [30]. Apart from surface morphology, fractal analysis can also help to study solvent-mediated phase changes of pharmaceuticals. Thus, hydrate formation on the surface of a solid in an aqueous medium has also been analyzed using binary images. In the course of hydrate conversion, clusters were forming and resulted finally in a Df of 1.85 that was not only interesting to describe the structure but also to reveal the underlying mechanism of hydrate nucleation and growth by diffusion [89].

Simple fractals can be generalized to a more versatile multifractal spectrum, which can be used to describe subtle geometrical features of a fractal object, which cannot be fully described by a single fractal dimension [36][38]. This multifractality is accessible through experiments or simulations via the moments of the distribution (Dq). Some of these multifractal moments are corresponding to quantities that have a particularly prominent role in percolation theory [66].

Important to note is that fractals provide a model framework that includes percolation theory. There are further applications to solid dosage forms for example regarding drug dissolution or to describe morphological or topological features of a solid formulation by mapping of the structure including information related to shape, mechanical, and further material properties [27][30][90][91]. Fractal physics (and in particular as described by percolation theory) demonstrates that a small perturbation of microstructural details (in a critical range) can lead to substantial macroscopic changes of the system properties [86].

The understanding provided by fractal geometry is based on the paths of microstructural change, and this is governed by the spatial distribution of topological events. A system component can, on the level of the microstructure be uniformly distributed in space or it can be aggregated into clusters [67][92]. Thus, clusters with diverse shapes and sizes spread in random directions and lead to geometrically irregular bulk structures and surfaces [93]. The initial stage of cluster formation is known as nucleation and is followed by densification and smoothing of the initial mass fractal structures. At this point, the system forms self-similar structures over wide spatial ranges. Physical porous objects typically exhibit pores (or solid particle structures) of almost all sizes, which can be evaluated by the box-counting method to quantify porous channels and surface structure [37] and be described either by a single fractal or by multifractal dimensions (Fig. 4) [68][94].

The continuation of the process and the forward of the cluster aggregation is related to the type of particles and the input energy in a system. Such aggregation can lead to self-similar clusters and upon further densification, clusters start to interpenetrate, which may follow the principles of percolation theory [95]. Compared to a random distribution, an aggregated system has more "free space" and hence the diffusion kinetics of such a system may be different [70], [93].
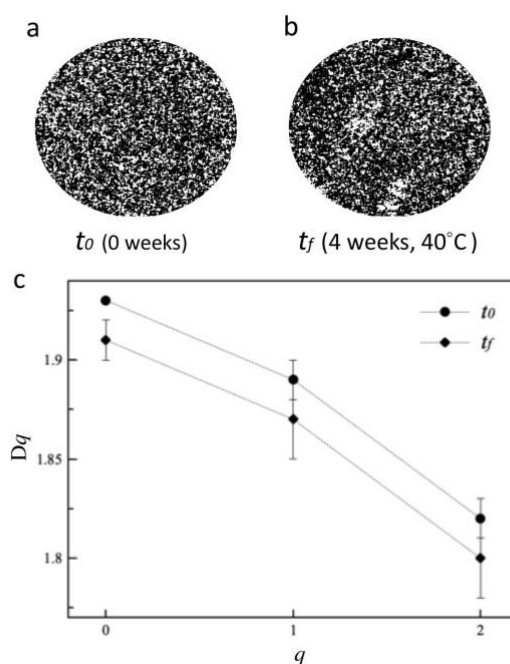

Fig. 4. (a) Example of typical two-dimensional EDS binary pictures microstructure seen by EDS of a binary mixture of Felodipine and HPMCAS-LF at initial time (t_0). (b) Microstructure evaluation of binary mixture after 4 weeks at 40∘C (t_f) showing drug-rich phase (white domains). (c) Generalized dimension Dq spectrum over the [0;2] moment q range for t_0 and t_f. Figure adapted from (Abreu-Villela et al., 2018).

There is practical relevance for the case where components of a system are above the percolation threshold and thereby form independent system spanning clusters that are interpenetrating each other [70][93]. The interpenetrating process of clusters influences the topological properties of the whole system [96]. Below the percolation threshold, the structure represents a complex system of finite clusters from which a (fractal) percolating cluster emerges. Further, above a percolation threshold, densification of interpenetrating clusters leads to smaller and smaller length scales (i.e. correlation lengths) below which heterogeneity is observed. Upon such densification, the percolating cluster ceases to be fractal, becomes homogeneous and acquires dimensionality of the embedding space on scales that are bigger than the correlation length. [73][96]. Thus, combined insights from fractal geometry (and percolation theory in particular) provide a geometry-based framework to better understand physical systems that can be idealized based on cluster aggregation [92][97]. Thinking of tablets, clusters of a mathematical model can hold for different physical substructures of the

compact such as, for example, pores, or primary particles, or even a mesoscale of an aggregated component in mixtures depending on which system and tablet property is considered.

Hence the science of solid formulations is a complex area in pharmaceutical technology. Unlike simple solutions, a molecular understanding and modelling is currently not given to an extent that it can be 'translated' into laws for particles and their compacted tablets [98]. Scaling law models provide an opportunity to connect the microscale to the macroscale [69]. Such scaling laws are part of fractal physics as well as percolation theory and provide at least some mechanistic description. This means, for example, that a power law of percolation may come with a theoretically known percolation threshold and exponent, but the proportionality constant is not predictable by theory.

3.4. QbD perspective: contributions of percolation theory and fractal geometry

The percolation theory and fractal geometry approaches are promising to describe solid formulations and especially mixtures with different components such as drug and excipients. Understanding of formulations is important to identify for example critical points in the design of formulations and in a process for effective development. Fig. 5 illustrates a path for implementation of QbD approach.

Percolation thresholds should be known in order to define the Design space of a formulation that exhibits a critical range of a quality attributes. These thresholds hold for critical volume of mass ratios and in their vicinity, small changes generally have pronounced effects on either process or final quality attributes. Its case of tablets this could mean effects on, for example lamination, capping, and changes in tensile strength of the compacts. Interesting is the view that data-mining acquired from percolation theory could be a useful tool to predict the manufacturing route sensitivity [99] providing a science-based approach for the estimation of the Design space [56]. One example can be found in the field of sustained release matrix tablets for which the knowledge of the critical concentrations of drug and matrix former polymer is vital to obtain formulations with a robust sustained release behavior [56]. Critical concentrations of a tablet component have also shown to be relevant for designing binary or multicomponent pharmaceutical tablets of to achieve sufficient mechanical strength [100].

Interesting is further another example of binary drug-excipient mixtures for which a critical concentration of drug was identified, above which powder mixtures showed highly erratic flow [101]. The same study further showed that such high drug concentrations close and above the critical point were leading to a sharp increase in dosing weight variation of the final dosage form (i.e. capsule). [102] investigated powder blend behavior and segregation tendency by considering percolation threshold. Another interesting field is application of percolation theory in the field of pharmaceutical colloids. For example, phase transitions of liposomes and the medium properties were evaluated in the framework of percolation threshold [103]. There are many possible applications of fractals in the field of pharmaceutical nano delivery systems. This is relevant not only for nano systems as final dosage form but also regarding colloids that emerge after oral administration of solid dosage forms as for example solid dispersions. Such nano systems could also serve as intermediate products for a solid dosage form development [28][35]. The fractal approach was also been proposed as a complementary tool for evaluation of the morphological characteristics of nanosimilar products [104]. Furthermore, fractals proved to be helpful to evaluate the stability of liposomal systems [105]. These different studies of pharmaceutical nano systems suggest that fractal aspects need to be studied to design quality into colloidal drug delivery systems.
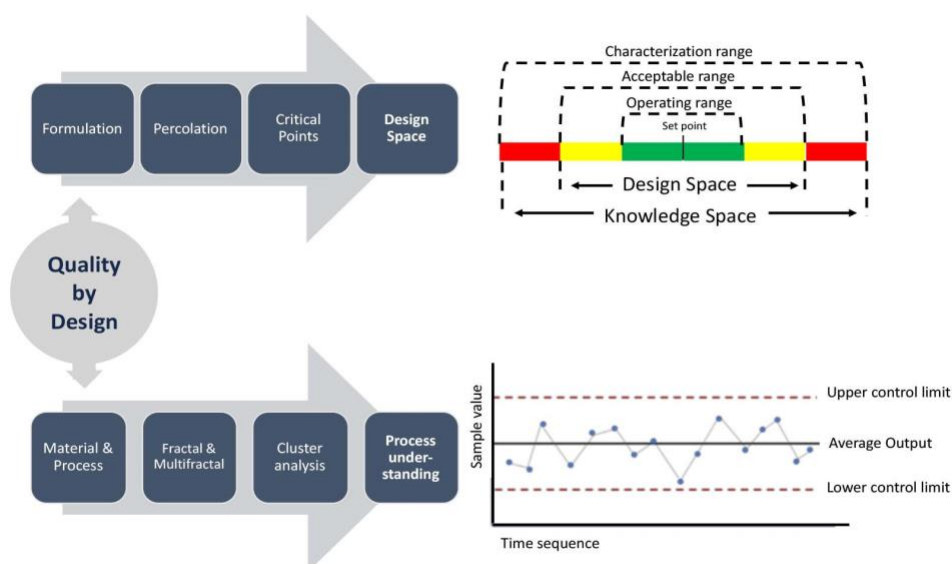

Fig. 5. Main steps of QbD approach for design space and process understanding from formulation (percolation) and process (fractal & multifractal) characterization and their impact in quality throughout the development and manufacturing process of pharmaceutical products

Interactions of colloidal clusters play also a role in the field of nanocomposites. The distribution of silica nanoparticles in nanocomposites and its impact on the mechanical

properties of the system was also evaluated based on the concept of percolation [106][107]. Such applications in pharmaceutically relevant material sciences are especially promising. This may not only target material properties for drug delivery systems directly but is also relevant for designing membranes that are used ubiquitously in the pharmaceutical sciences. For example, the influence of the particle diameter on the percolation threshold in a membrane formed by spherical nanoparticles has been studied using a computer simulation program [108]. These results are in agreement with the experimentally found by our research group more than two decades ago [109][110] showing a decrease in the percolation threshold as the particle diameter increases.

Other more recent pharmaceutical work on amorphous solid dispersions revealed that excipient and drug clusters are better described by multifractal formalism than by a single fractal dimension [36][111]. The findings based on imaging techniques were shown to impact quality attributes such as mechanical strength and physical stability of the analyzed solid dispersions [53][112].

In conclusion, the rough topography or complex pores structure of solid dosage forms is not directly predicted by any model with a Gaussian distribution. However, fractal geometry, the multifractal approach and the models based on percolation theory have been proposed to describe the statistical properties of such surfaces and bulk morphologies. Percolation theory has been successfully applied for identification of critical concentrations of formulations that impact on critical process and quality attributes of the final dosage form.

The given examples and the theoretical considerations demonstrate how promising the concepts of fractal geometry and percolation theory are to address the QbD philosophy to bring important benefit for optimization of formulations. Particular advantages of this approach are the sound mechanistic basis of taking the microstructure into account that is mostly a "black box" in classical DoE approaches. Such statistical designs are, on the other hand, very economical in terms of experimental investment, but it seems best to combine purely correlative knowledge based on for example DoE with more mechanistic approaches as presented in this review.

Chapter 4

Electron microscopy/energy dispersive X-ray spectroscopy of drug distribution in solid dispersions and interpretation by multifractal geometry

Summary

Much contemporary research of poorly water-soluble drugs focuses on amorphous solid dispersions (SDs) for oral drug delivery. Recently, a multifractal formalism has been introduced to describe the distribution of an inorganic carrier in SDs. The present work attempts to directly image model drugs by means of scanning electron microscopy and energy dispersive X-ray spectroscopy. The compounds amlodipine, felodipine, glyburide, and indomethacin, which include halogens to enable sufficient scattering in energy dispersive X-ray spectroscopy, were employed to prepare SDs with hydroxypropyl methylcellulose acetate succinate (HPMCAS) by using a microwave method. Following chemical imaging, it was demonstrated that drug distribution was best described by multifractals, which was clearly superior to a monofractal assumption. The obtained fractal dimensions were influenced by drug

loading and it was possible to detect microstructural changes upon addition of the plasticizer urea. Accordingly, the multifractal approach bears much potential to better explore the analytical results of chemical formulation imaging. Insights can be gained from the microstructural organization of SDs, which is interesting to further study formulation and process factors as well as physical stability.

4.1. Introduction

Solid dispersions (SDs) provide an important formulation approach to improve dissolution and apparent solubility of an active pharmaceutical ingredient (API) that is poorly water-soluble [4][6][47]. However, SDs also come with some technical challenges such as thermodynamic instability. An increased understanding of drug properties and physicochemical interactions with matrix components has been achieved in recent years, which is lever-aging such development risks [1][10][48][49]. Among the different analytical tools, imaging methods have become increasingly important nowadays. A potential phase separation has been studied, for example, by cross-polarized imaging, vibrational spectroscopic imaging or atomic force microscopy (AFM) [17][50][51]. Depending on the method, such imaging of a phase separation may provide a clear visual result. However, direct insight from looking at obtained images is unfortunately often not achieved. Imaging may just show a complex cluster structure that is difficult to compare and interpret at given length scales. Few studies have, for example, investigated microstructures by means of AFM at a size range of nanometers [118]. It is in this respect indifferent, whether an obtained cluster structure was calculated by a chemometric method or if a cluster distribution was obtained directly from a given imaging method.

A lack of direct interpretation by the naked eye can be unsatisfying. The approach of a simple cluster statistics by determining their size and number can be rather tedious, especially in absence of an automated computer program. Moreover, a comparison of mean cluster sizes may offer only limited sample differentiation [20]. There is an obvious need of advanced data processing once images are obtained to extract relevant structural information from solid dosage forms. Such data processing can be geared towards for example homogeneity [19][20][53]. However, it may be even more attractive to apply a mathematical model for heterogeneous physical structures such as fractals [120]. Even though there are many applications of fractals in pharmaceutics [35], there are fewer reports in which fractals are

applied to dynamic imaging of dosage forms [89]. Thus, fractals appear to be rather underexploited for imaging of pharmaceutical dosage forms compared to, for example, medical imaging [121]. The fractal approach offers a physical model, which enables more than just sample comparison as it bears potential to gain mechanistic insights into how a microstructure has been generated. Recently, multifractal formalism was introduced to pharmaceutics to analyze data from electron microscopy and energy dispersive X-ray spectroscopy [36][57]. This pioneer work of microstructural analysis focused on inorganic carrier distribution in pharmaceutical extrudates and consequences on mechanical hardness.

The present work attempts for the first time to employ multi-fractals for analysis of the drug distribution in SDs. Thus, different APIs were selected which include halogens to enable sufficient scattering in energy dispersive X-ray spectroscopy. The model polymer hydroxypropyl methylcellulose acetate succinate of grade "LF" (HPMCAS-LF) was used as a carrier matrix. This grade has relatively higher succinoyl substitutions (14–18%) as compared the others grades, i.e. MF (10–14%), and HF (4–8%) [122], which affects hydrophilicity of a solid dispersion [123]. There was a specific aim to study effects of the formulation on the obtained fractal dimensions. Herein, drug load was of interest but also the addition of urea because this excipient has shown promise for reducing the manufacture temperature as well as to improve drug release from SDs [124].

4.2. Materials and methods

4.2.1. Materials

HPMCAS-LF (Shin-Etsu AQOAT$^®$) was kindly donated by Shin-Etsu Chemical Co. Ltd. (Tokyo, Japan). Amlodipine (AML) and glyburide (GLY) were purchased from Molekula Ltd. (Newcastle Upon Tyne, UK), felodipine (FEL) and indomethacine (IND) from Kemprotec Ltd. (Smailthorn, Cumbria, UK), whereas urea was purchased from Sigma-Aldrich (St. Louis, Missouri, USA). Physicochemical properties of the AML, FEL, GLY and IND are showed in Table 2.

Table 2

Physicochemical API properties.

Compound	Molecular weight (g/mol)[a]	Melting Temperature (°C)[b]	log$P$[a]	pKa[a]	Water solubility (mg/mL) at 25 °C[a]	Total solubility parameter (MPa)$^{1/2}$ [c]
Amlodipine	408.8	140.5	3	9.45	0.0074	22.5
Felodipine	384.3	144	3.86	5.39	0.0072	23.0
Glyburide	494	173.5	4.7	4.32	0.0021	24.7
Indomethacine	356.7	161.5	4.27	4.5	0.0024	23.5

[a] Molecular weight, partition coefficient log$P$, dissociation constant pKa and predicted water solubility are taken from the DrugBank database (https://www.drugbank.ca/).

[b] Melting temperature values taken as the average maximum temperature of melting endotherm for three samples.

[c] Hansen Solubility parameter estimated by the software Molecular Modeling Pro V.6.2.6 (Norgwyn Montgomery Software Inc., North Wales, PA).

4.2.2. Methods

4.2.2.1. Preparation of physical mixtures and solid dispersions by microwave heating

The present work was making use of a microwave irradiation (MW) preparation method that was similar to what has been reported before [124]. Defined amounts of the different components (i.e. 1 g) were mixed at room temperature at various weight ratios (Table 3), water was added, and the mixtures were stirred at 700 rpm for 15 min.

The obtained homogeneous suspensions were transferred into a vial containing a magnetic stir bar. SDs were produced by using microwave assistance in a Biotage Initiator system (Biotage, LLC; Charlotte, NC, USA) operated and controlled by the software. The samples were heated to 120° C with a power of 75 W during 10 min and later cooled to room temperature before being dried and freeze/milled (Spex Sample Preparation; Metuchen, New Jersey, USA). Following milling, no visual changes were observed except for an intended size reduction and particle uniformity. Subsequently, samples were stored in a desiccator until further investigations.

4.2.2.2. X-ray powder diffraction

X-ray powder diffractograms (XRPD) were determined for physical mixtures (PM) as well as MW formulations. A D2 Phaser diffractometer (Bruker AXS GmbH, Karlsruhe,

Germany) was employed that was equipped with a Co–2 K KFL diffraction tube configured and a 1D- Lynxeye detector and with a Fe filter. The applied voltage and current were 30 kV and 10 mA, respectively. Diffraction patterns were obtained using a step width of 0.02∘ C with a detector resolution in 2 between 6 and 40° and a scan speed of 2s/step at room temperature. Data interpretation was per-formed by using the EVA program (Bruker AXS GmbH, Karlsruhe, Germany).

4.2.2.3. Preparation of compacts

Powders of MW formulations were compressed with a tablet press to facilitate a smooth and flat sample surface for subsequent chemical imaging. 100 mg of SD and 7 mm flat faced punch was used as tooling for a manual compaction using a hydraulic XP1 press (Korsch AG, Berlin, Germany).

4.2.2.4. Scanning electron microscopy and energy-dispersive X-ray spectroscopy

The samples were placed on double-side adhesive carbon tabs and the surface of the compacts was coated with gold under argon vacuum with a Sputter Coater SC7620 (Quorum Technologies Ltd., Kent, UK), which was observed with a Scanning electron microscopy (SEM) TM3030 PLUS (Hitachi High-Technologies Corporation, Tokyo, Japan). A voltage of 15 kV and 150× magnification was used. Energy-dispersive X-ray spectroscopy (EDS) analysis was based on a Quantax 70 system software (Bruker Nano GmbH, Berlin, Germany) consisting of an X Flash Min SVE signal processing unit, a scan generator and Megalink interface together with an X Flash silicon drift detector 410/30H (Bruker Nano GmbH, Berlin, Germany). Samples were scanned during 5 min to map the distribution of APIs that contain chloride (Cl) atoms for comparatively higher X-ray scattering intensity.

4.2.2.5. Image processing and multifractal analysis

Once the images of the studied object were captured, they were processed using Adobe Photoshop Creative cloud software (Adobe Systems, San Jose, California, USA). Each picture was converted to binary images of 1024×768 pixels for which black was set as background. A predetermined image size avoids artifacts, which may occur when boxes do not entirely cover the image at the borders. The Image J software (National Institutes of Health, Bethesda,

Maryland, USA) plugin image analysis tool FracLac was employed to perform the box counting multifractal analysis. The number of grid orientations, the maximum box size as% of pixels, and the moment q range were set to 4, 60, and [-5; 5], respectively. A power series of box sizes was selected with 2, 4, 16, 64 and 256 pixels. Three compacts of each formulation were analyzed.

A Box counting method to cover a 2-D image was used for calculation of fractal dimensions. Thus, successive grids of sizes ε were used for this purpose. The number N of boxes containing at least one pixel of the observed object was recorded and the procedure was repeated with different grids to compute fractal dimensions [54][56][61]. In a monofractal system, the object measured is assumed to have a structure, which is repeated over different spatial scales. However, complex structures may not entirely be described by monofractal analysis. In multifractal analysis sets can also be characterized trough the scaling of qth order moments of Pi distribution. The box counting method determines the partition function X (q, ε), which can be considered as the probability to find the object in the ith box for different moments q varying in the $[-\infty; +\infty]$ interval. The generalized dimensions are obtained as the slope of the portion function over box size, both taken as logarithms (Equation reference [36][56]). This method is knowns as the method of moments, D_q.

D_q can be viewed as the "deformation parameter" of variability degrees and q extracts different features of the distribution. Particularly interesting are D_0, D_1 and D_2, where D_0 refers to the "capacity" dimension that describes how a multifractal system covers the observed domain. The parameter D_1 is called a dimension of Shannon entropy that characterizes the degree of disorder in a distribution. Finally, D_2 hold for the "correlation" dimension, which indicates a degree of clustering. If the values for D_0, D_1, and D_2 are for example rather high, this would suggest a high degree of space coverage, high disorder, and low clustering level, respectively [126]. In case of monofractal self-similarity, $D_0 = D_1 = D_2$, whereas different values $D_2 \leq D_1 \leq D_0$ indicate a multifractal system [127].

4.2.2.6. Statistical analysis

STATGRAPHICS Centurion XVI ed. Professional (V. 16.1.15) from Statpoint Technologies Inc. (Warranton, Virginia, USA) was used to evaluate analysis of the variance (ANOVA). Tukey's honest significant difference test was used for means comparison of

generalized multifractal dimensions D_0, D_1, and D_2. For all the statistical tests, a p-value <0.05 was considered significant.

4.3. Results and discussion

4.3.1. Preparation of solid dispersions and X-ray diffraction

SDs can be prepared by a solvent method or based on application of heat, as it is the case for hot-melt extrusion (HME) or a MW method. The latter method is attractive due to its simplicity but not all polymers can be processed in this way and lack of shear forces compared to HME may require elevated manufacturing temperatures [62][63]. This is one of the reasons why urea is an interesting excipient for MW because it bears potential to reduce manufacturing temperature [124]. However, all formulations of the present study (Table 3) were processed without any complications. XRPD (Fig. 6) of the physical mixture (PM) showed distinct visible peaks that were pointing to drug that remained crystalline as expected. By contrast, all the formulation produced in the microwave showed only a halo, so the absence of peaks indicated the successful conversion of the APIs to their amorphous forms in the SDs. The macroscopic appearance of the different SDs of IND was transparent and suggested the likely formation of glass solutions. By contrast, the other amorphous drug formulations exhibited different degrees of macroscopic turbidity that together with the XRPD results indicated the formation of glass suspensions [10].

Table 3

Composition of the different solid dispersions.

	Drug %(w/w)	HPMCAS-LF %(w/w)	Urea %(w/w)	Formulation
AML	5	95		AML5
AML	7.5	92.5		AML7.5
AML	10	90		AML10
AML	10	85	5	AML10U
FEL	5	95		FEL5
FEL	7.5	92.5		FEL7.5
FEL	10	90		FEL10
FEL	10	85	5	FEL10U
GLY	5	95		GLY5
GLY	7.5	92.5		GLY7.5
GLY	10	90		GLY10
GLY	10	85	5	GLY10U

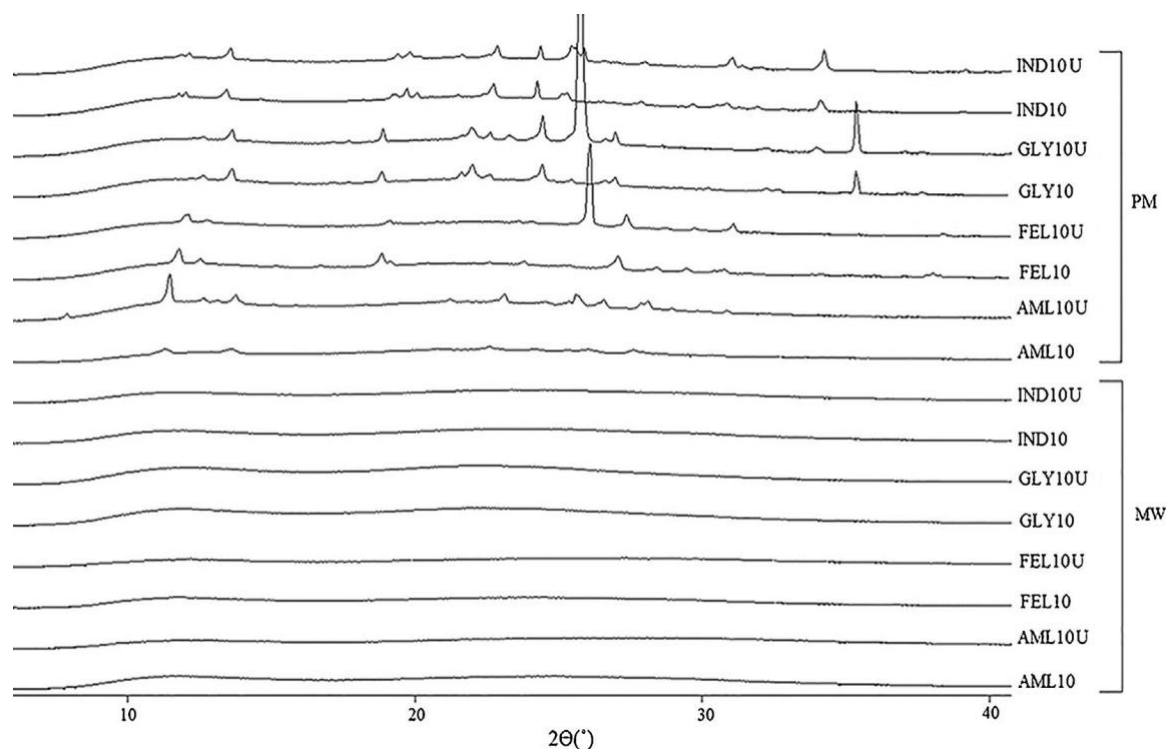| IND | 5 | 95 | | IND5 |
IND	7.5	92.5		IND7.5
IND	10	90		IND10
IND	10	85	5	IND10U

Fig. 6. Power X-ray diffractograms of 90/10% (w/w) HPMCAS-LF/API PM, 85/10/5% (w/w) HPMCAS-LF/API/U PM, 90/10% (w/w) HPMCAS-LF/API MW, 85/10/5% (w/w) HPMCAS-LF/API/U MW, where the APIs are AML, FEL, GLY, IND. Details are explained in the text.

4.3.2. Compact surface mapping by energy-dispersive X-ray spectroscopy

It is known from the literature that SEM-EDS is the mostly used technique for representation of elemental composition from micro-scale surface, with a detection limit of approximately 0.1% [62][63]. The overall spatial resolution of the method is limited by the focused beam and the scattering of elastic or inelastic electrons. If the beam is finely focused, it provides a high spatial resolution even for mapping bulk species in the range of 10 keV to 30 keV [128]. Since SEM-EDS application focus on elemental specific localization and distribution on the compact surface [129], we selected model drugs that contain Cl atoms as they are generally well detected by SEM-EDS given that their elevated atomic number facilitates relatively higher X-ray scattering intensity in organic molecules. Representative SEM and the corresponding EDS-2D binary pictures of drug formulations are shown in Fig. 7. The light pixels of the latter 2D representations were specific for detected Cl atoms that were

only present in the drug molecules. From those micrographs, it becomes apparent that the drugs were not homogeneously dispersed throughout the samples. At first sight, SEM-EDS images suggest a complex structure of clusters, but the absence of comparatively large domain formation shows that there was no pronounced phase separation given in the studied SDs.
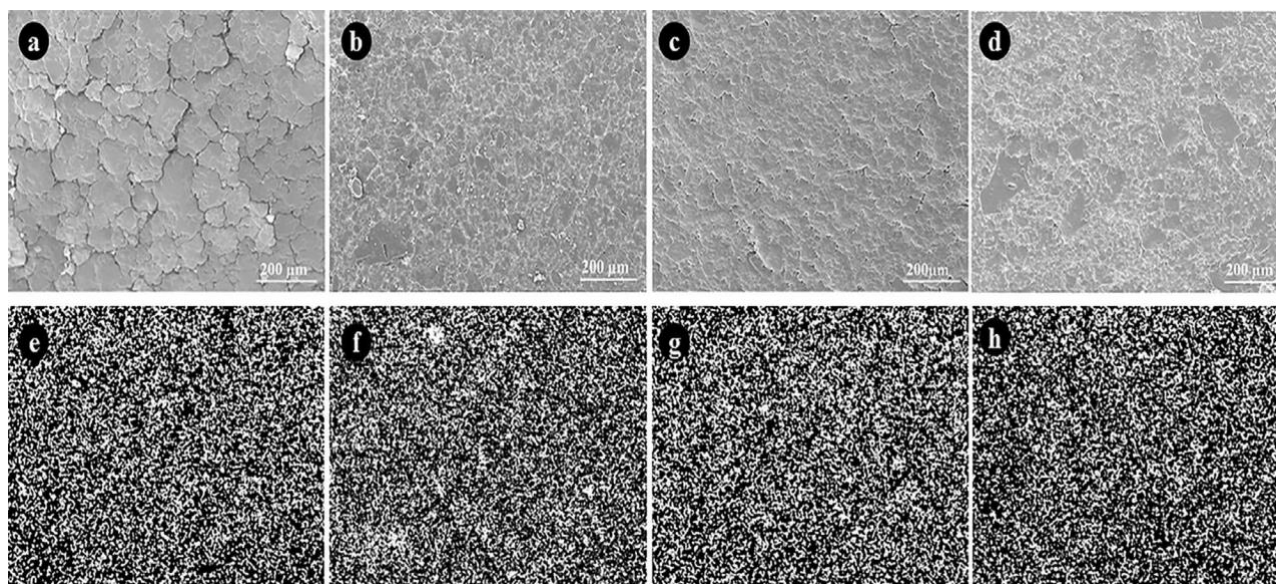
Fig. 7. SEM (a, b, c, d) and corresponding EDS 2-D binary pictures (e, f, g, h) of Cl distribution in tablets containing 90/10% (w/w) of HPMCAS-LF/API, where the APIs are AML (a, e), FEL (b, f), GLY (c, g) and IND (d, h).

4.3.3. Multifractal analysis

4.3.3.1. Image analysis

Inspecting the Cl distribution on the 2D images by the naked eye can barely provide insights beyond the finding of an absent larger-scale phase separation. For a more refined cluster analysis, this work introduced the multifractal approach to study drug distribution. This was employed as a tool to quantify the complexity and spatial heterogeneity of compound in SDs. It is of course important to recall that the 2D representations were images of a 3D topography [130] but the samples were comparatively flat, and the scaling approach of any fractal algorithm should enable a rather versatile use for drug distribution analysis.

4.3.3.2. Multifractal analysis of binary system

The multifractal approach as a cluster analysis was used to study SDs. It is known that drug can be incorporated differently in a matrix dependent on the type of amorphous formulation [6]. However, the categories in the literature such as glass solutions or glass suspensions are umbrella terms for systems that can be quite variable in their microstructure. Drug clusters can exhibit very different space coverage and the degree of disorder and level of clustering can show differences. In line with previous work on excipient distribution, a particular interest was therefore in the fractal dimensions D_0, D_1, and D_2 [112]. These obtained numbers are generally sufficient to thoroughly characterize a cluster structure. Space coverage ("capacity dimension") in a given domain is obtained by D_0, whereas D_1 ("information dimension") holds for a degree of disorder, and finally the correlation dimension D_2 characterizes the degree of clustering ("correlation dimension").

A first interest was to see whether results would be different among the model drugs studied (Table 2). AML and FEL have basic moieties, whereas GLY and IND are acidic drugs. All model compounds exhibit poor water solubility, they were selected in confined ranges of lipophilicity and solubility parameter, and an initial screening test revealed the suitability of these model com-pounds to produce SDs with HPMCAS-LF. As a result of the multifractal analysis, the evolution D_q versus q for the formulations AML10, FEL10, GLY10, and IND10 (in the range of moment $_q$ [-5; 5]) displayed sigma-shaped curves and D_q decreased with higher values of q. This shows that the multifractal approach does not introduce any unnecessary complication because the simpler monofractal model would be clearly inadequate, as it would assume a single constant fractal dimension along different values of q. It was interesting to investigate specific influences of given compounds on the multifractal dimensions. A more detailed view on D_0, D_1, and D_2 is given in Fig. 8 and the upper panels (a)-(d) to compare different drug loadings. Results suggest some effect of the compound as well as of its concentration on the microstructural features of the SDs. Fig. 8 (a-d) indicates for AML10, FEL10, GLY10, IND10 that rising drug concentrations increase the different dimensions thereby indicating a higher space coverage (D_0), higher dimension of disorder (D_1) and higher correlation dimension (D_2), which in turn suggests a lower degree of clustering. Current results bear interesting qualitative similarity with D_0, D_1, and D_2 values that were reported as multifractal results for the distribution of an inorganic carrier in hot melt extrudates [36].

The observed effect of compound and drug loading were also statistically analyzed at a reference drug load of 10% (w/w). A two-way ANOVA conducted and supported the view of

a significant API effect on D_0 (p = 0.0012) as well as a clear effect of drug load on the same dimension (p < 0.0001). Fig. 9 allows comparing the Tukey's 95% highest significant differences for the different drugs or concentrations, respectively. A most pronounced difference for the API type was between AML-FEL and FEL-IND. An interpretation of this result is that molecular interactions of the compound with HPMCAS would define a particular microstructure of how drug clusters form in a SDs.
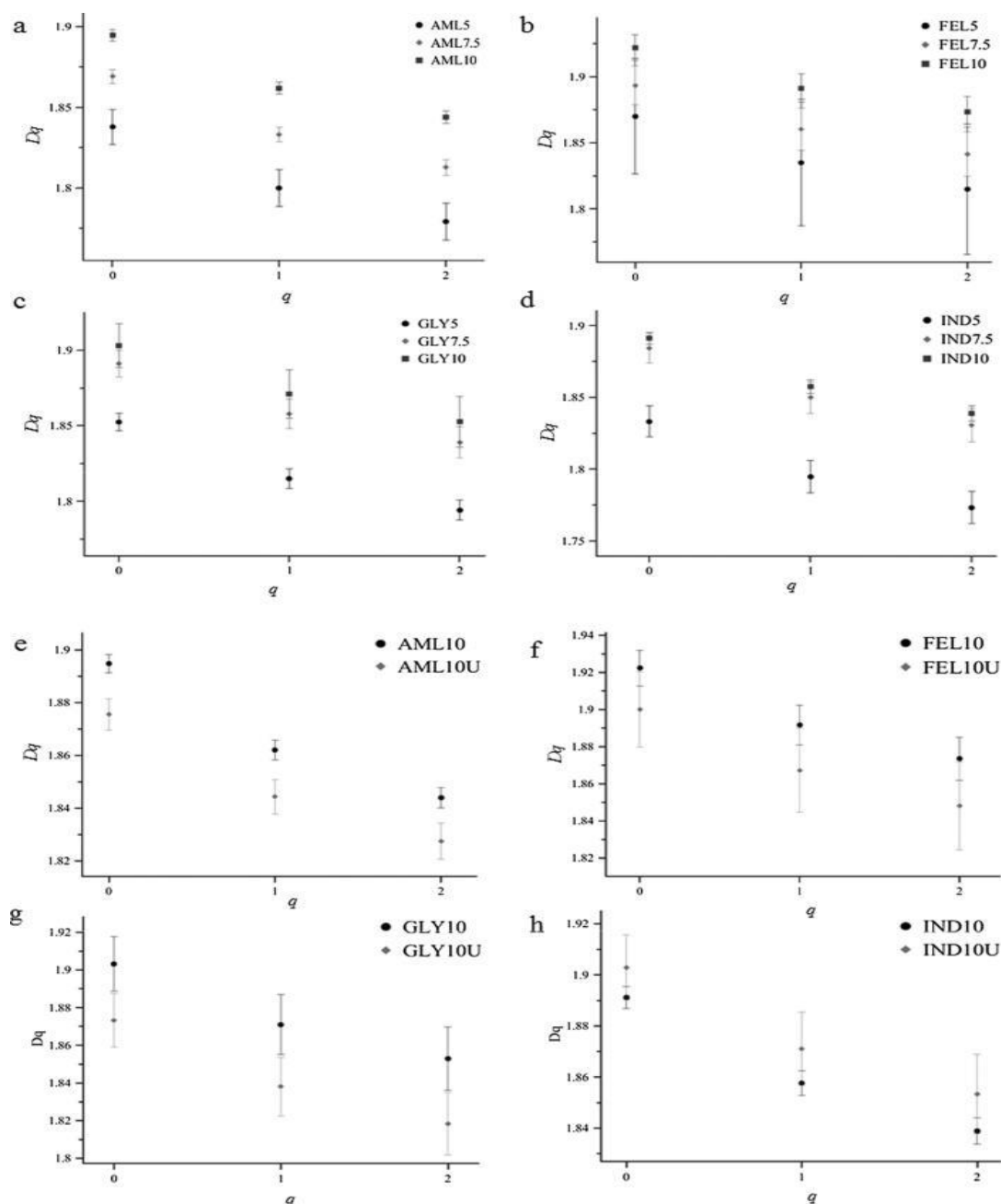

Fig. 8. Generalized dimension Dq spectrum over the [0;2] moment q range for solid dispersions. The upper four panels (a)-(d) show drug concentration effects, while the lower panels (e)-(h) display effects of added urea (5% w/w) at a constant drug load (10% w/w). Details are explained in the text: AML5, AML7.5, AML10 (a); FEL5, FEL7.5, FEL10 (b); GLY5, GLY7.5, GLY10 (c); IND5, IND7.5, IND10 (d); AML10, AML10U (e); FEL10, FEL10U (f); GLY10, GLY10U (g); IND10, IND10U (h).

The dimension D_1, and D_2 were also studied in a two-way ANOVA of the same factors and results were quite comparable with respect to obtained p-values. These values remained practically the same for D_1 as for D_0 (rounded for four digits after the comma). Regarding D_2, the effect of drug yielded a very similar p-value of 0.0014 for API type and again $p < 0.0001$ for drug loading. The qualitative differences among compounds were comparable with respect to D_0, D_1 and D_2. Thus, APIs were obviously affecting in their particular way the microstructure of the SDs even though the trends in changes of fractal dimensions were quite comparable.

The topic of drug distribution in amorphous dispersions has been also approached by molecular dynamics simulations (MD) that showed a non-uniform distribution of drug in a polymeric matrix [131]. MD simulations can not only analyze the drug aggregation and formation of supramolecular structures in a polymeric melt but also upon aqueous dispersion [132]. While such atomistic simulations are beneficial to learn about molecular drug-excipient interaction motifs, it is currently hardly possible to get quantitative information on the cluster structure of formulation components because this would require a substantial increase in computation resources. In the future, MD simulation results might be compared with findings of cluster analysis as studied by the multifractal approach.
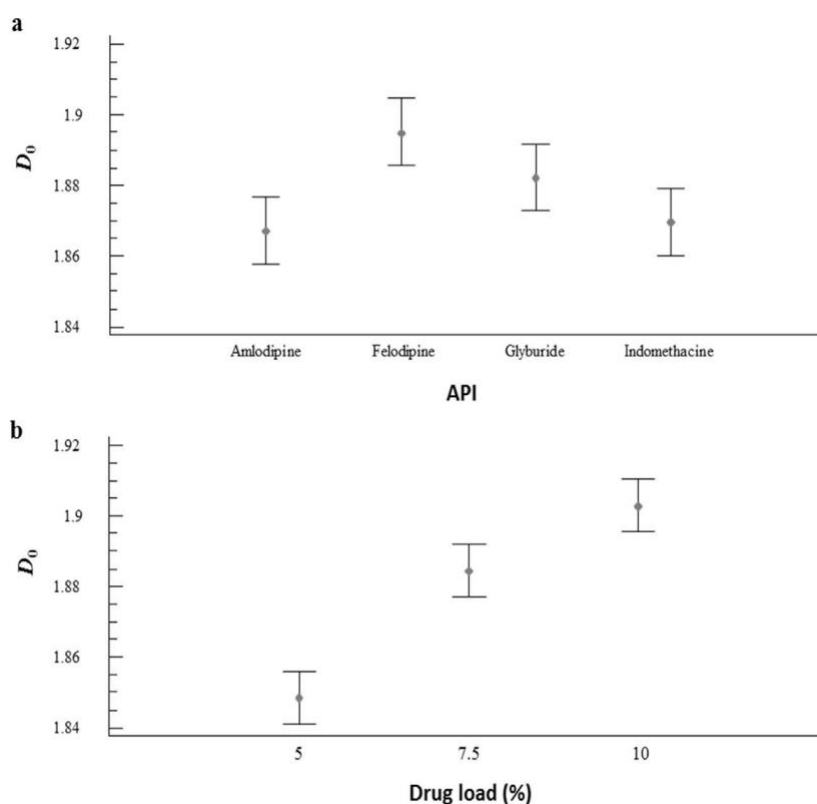
Fig. 9. Statistical means plot based on a two factor ANOVA how D0 is affected by the drug (10% w/w) in solid dispersion (a); and D0 as influenced by drug concentration (b). Tukey's highest significant differences (95%) are shown.

Interesting for an alternative technique of drug distribution analysis is a fluorescence study that was based on fluorescence resonance energy transfer (FRET) [133]. This technique had the disadvantage that only the distribution of fluorescence probe molecules could be studied but an interesting finding was the cluster nature of how model compounds were spatially distributed in the matrix. We found in the current work also a cluster structure of drug in the solid dispersions of IND, which appeared rather as glass solutions by their macroscopic appearance. The current analysis is of course a snapshot in time, so it is possible that initial nuclei of an amorphous-amorphous phase separation have already formed but were too small to be seen macroscopically. Further studies of such time-related changes [10] are of interest but would go beyond the scope of the current work.

The multifractal approach provides major benefits for chemical imaging of SDs because effects of formulation parameters can be detected in the microstructure. This was in line with prior work that focused on the distribution of an excipient in SDs [89]. Any simple assumption of a homogenous drug distribution in SDs or a distribution that can be described as a monofractal system falls short in light of the present results. A proper understanding of such heterogeneous drug distributions obviously requires studying different length scales.

4.3.3.3. Multifractal analysis of ternary system

To extend the multifractal approach to more complex systems, ternary mixtures with a concentration of 5%w/w urea were analyzed. The latter additive is of interest from a formulators perspective regarding a potential reduction of manufacturing temperature and it has shown some promise to enhance drug release [124]. For the present work, a primary objective was to see how the presence or urea would perturb drug distribution in the SD and how these microstructural effects would be reflected in terms of the fractal dimensions.

The more complex ternary systems were viewed as simple mixtures of API with a matrix of excipients. For chemical imaging, this approach results in "pseudo-binary images" [134] that depict drug in a matrix of additives. Fig. 8 (e)-(h) indicated multifractal analysis of API distribution indicating a lower generalized dimension on formulation with urea, corresponding to a lower space coverage (D_0), lower heterogeneity (D_1) and higher clustering level (D_2). In contrast to all other APIs, SDs of IND and polymer had lower values of D_0, D_1 and D_2 than IND formulations with added urea.

An ANOVA of the formulations with 5% (w/w) urea and their corresponding reference systems without urea supported the view of a significant drug effect on, for example, D_0 (p = 0.0212) and a significant effect of adding urea (p = 0.0183). These effects were also found to be significant regarding D_1 (p = 0.0325 for the effect of drug type and p = 0.0261 for that of urea). The corresponding ANOVA for D_2 has revealed a borderline effect for the drug (p = 0.0512), while the significance level was again reached for the urea effect (p = 0.0336).

From a mechanistic perspective, urea could have different effects. Owing to its particular structure, urea has the ability to interfere with hydrogen bonding. An influence of urea on hydrogen bonding patterns in solid dispersions is therefore interesting but would require additional spectroscopic studies for clarification. There could be also general effects of urea on the cluster structure so that a simple dilution of polymer in the pseudo-binary images could have played a role in the observed fractal dimensions of the ternary mixtures.

4.4. Conclusions

SEM-EDS application on the surface of solid dispersion samples showed a suitable detection of the different model drugs that contained Cl. This multifractal analysis of SEM-EDS images proved to be reproducible and robust. It provided the means to assign numbers to a heterogeneous structure as observed from chemical imaging. The present work attempted for the first time a multifractal analysis of drug distribution in SDs and proved the superiority compared to any model description that is based on a single fractal dimension. The analysis allowed detecting effects of different drug types and their concentration on the microstructure. Notable was that the promising additive urea showed clear effects on the different fractal dimensions. Chemical imaging together with the multifractal approach bears much promise from a theoretical as well as practical perspective. Complex cluster structures can be analyzed, and structural insights can be gained that may help to better under-stand the performance of a SD or of another type of pharmaceutical dosage form. Future work could study time-effects such as physical changes upon storage and the effects of excipient grades as well as manufacturing techniques on drug cluster formation.

Early stages of drug crystallization from amorphous solid dispersion via fractal analysis based on chemical imaging [3]

Summary

Early stages of crystallization from amorphous solid dispersion (ASD) are typically not detected by means of standard methods like powder X-ray diffraction (XRPD). The aim of this study is therefore to evaluate if fractal analysis based on energy dispersive X-ray imaging can provide the means to identify early signs of physical instability. ASDs of the poorly water-soluble compound, felodipine (FEL) were prepared by solvent evaporation using different grades of HPMCAS, at 50 wt% drug loading. Samples were stored at accelerated conditions of 40 °C. Scanning electron microscopy equipped with an energy-dispersive X-ray spectroscopy (SEM-EDS) was used for elemental mapping of tablet surfaces. Comparative data were generated with a standard XRPD and with more sensitive methods for detection of early instability, i.e. laser scanning confocal microscopy (LSM) and atomic force microscopy (AFM). The SEM-EDS identified changes of drug-rich domains that were confirmed by LSM

and AFM. Early changes in drug clusters were also revealed by a multifractal analysis that indicated a beginning phase separation and drug crystallization. Therefore, the presented fractal cluster analysis based on chemical imaging bears much promise as a new method to detect early signs of physical instability in ASD, which is of great relevance for pharmaceutical development.

5.1. Introduction

Amorphous solid dispersion (ASD) has become an established oral delivery technique to formulate poorly water-soluble drugs [1][7][9]. Given the large number of papers that are published on solid dispersions, it is rather surprising that there are not many more of these products on the pharmaceutical market [115]. One of the main reasons is that ASDs are metastable systems and bear the risk of physical instability during their shelf life. Drug crystallization can occur depending on the history of an amorphous product and on given conditions [135]. Particularly critical is storage at elevated temperature and moisture leading eventually to phase separation and crystallization, which means a loss of biopharmaceutical advantages using ASD [14][72][73]. The molecular processes of phase separation as well as crystallization from amorphous material are complex and mobility in the glass state plays an important role. Relaxation of amorphous materials take place on different time scales from primary diffusive (α-relaxation) to secondary local relaxation such as Johari-Goldstein relaxations (β-relaxation). While α-relaxation becomes very slow in the glass state, it is mostly the secondary relaxations that are relevant for crystallization from amorphous state [11]–[13]. Once crystallization starts, it continues to reduce the system's free energy [15][74]. Thus, thermo- dynamics is the driver for physical change and molecular mobility is a facilitator, while surface effects can act as modulators, and heterogeneities as amplifiers of crystallization [18].

A standard method to detect and characterize crystalline material is X-ray powder diffraction (XRPD) but like with other conventional methods such as differential scanning calorimetry, it is challenging to detect small amounts of crystalline material. Such small amounts can be already present following manufacture of an amorphous product or they are generated as initial instability but either ways, such crystallites can negatively affect kinetic stability of ASDs [15][74].

Interesting for detection of crystalline material are imaging techniques that can be based on different physical principles. Since amorphous formulations are typically multi-component systems, chemical image has the advantage that an active pharmaceutical ingredient (API) is differentiated from excipients. Any chemical imaging involves a sophisticated analytical technique for acquisition of images and spectra that contain the chemical information [21], which typically enables spatial distribution of one or all formulation components [22]. Images can be acquired at the surface and in the bulk by electron microscopy, such as, transmission electron microscopy (TEM) and scanning electron microscopy (SEM) with energy dispersive X-ray spectroscopy (EDS) [23][24]. Important are also vibrational spectroscopic techniques with appropriate optics, such as Raman [21][25][26], near infrared (NIR), or terahertz spectroscopy [15].

It is critical for any imaging technique how the large amounts of data are evaluated. Suitable algorithms such as modern chemometric methods can be applied to extract useful information from otherwise just large and incomprehensible data sets [21]. An algorithmic topic in its own right is how clusters are analyzed in images since a naked eye is not capable of detecting any subtle changes of an imaged micro- structure. Promising for any such cluster analysis is fractal geometry. This approach was pioneered by Mandelbrot and does not use classical geometry to describe physical objects [28]. Fractal geometry has been applied in pharmaceutics, for example, to describe a solvent-mediated formation of a drug hydrate [89]. However, a single fractal dimension is often not sufficient to adequately describe a complex heterogeneous system. A more generalized mathematical concept is given by multifractal analysis, which decomposes the self-similar measures into intertwined fractal sets that describe the variations from the average in heterogeneous systems [40].

Recently, the multifractal formalism was introduced in solid dispersion technology to describe the spatial distribution of an inorganic carrier [36]. In a subsequent work, the distribution of different drugs in ASDs was revealed to have a multifractal character [111]. The mathematical formalism was found to model adequately the heterogeneous nature of drug clusters in ASD and a next step would be to study changes over time. The hypothesis of the present work is that multifractal analysis based on chemical imaging can proof utility in analyzing early stages of physical instability. Thus, felodipine (FEL) was used as model drug in solid dispersions with the polymer hydroxypropyl methylcellulose acetate succinate (HPMCAS). The different grades LF and HF were used with 14–18% and 4–8% of succinoyl

substitutions, respectively [122]. ASDs of FEL/HPMCAS were analyzed topographically by SEM-EDS as a chemical imaging technique, which provided the basis for multifractal analysis. To have a comparison with other known sensitive methods, samples were also studied by laser scanning confocal microscopy (LSM) and atomic force microscopy (AFM).

5.2. Materials and methods

5.2.1. Materials

Felodipine (FEL) was purchased from Kemprotec Ltd. (Smailthorn, Cumbria, UK) and the different grades of HPMCAS (Shin-Etsu AQOAT®, Type LF and HF) were a generous gift from Shin-Etsu Chemical Co. Ltd. (Tokyo, Japan). Dichloromethane and methanol (HPLC grade) were procured from Sigma-Aldrich (St. Louis, Missouri, USA). The API chemical structure, as well as monomer units of the polymer, are given in Fig. 10. Particularly highlighted are chloride atoms regarding their selective detection by energy dispersive X-ray spectroscopy.
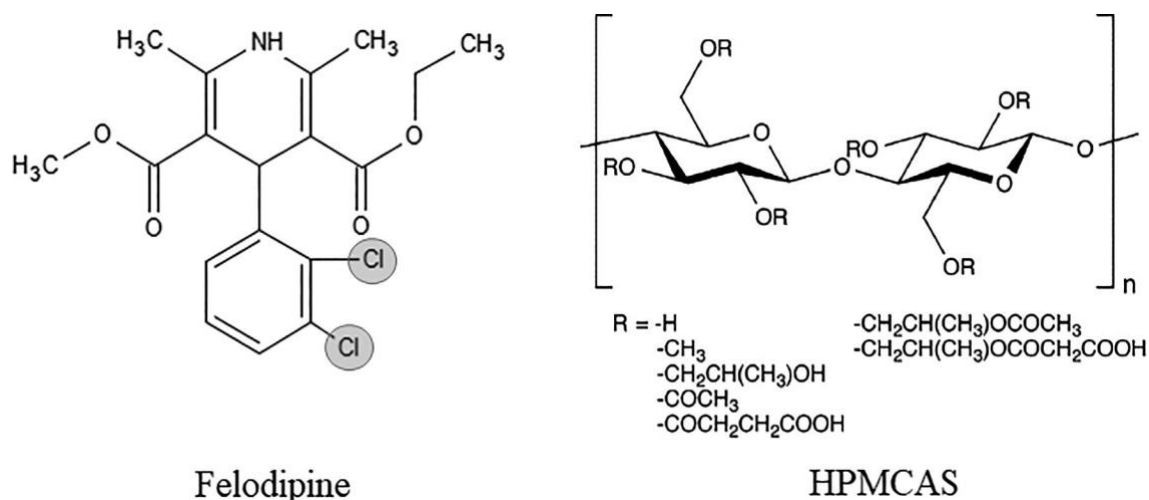
Fig. 10. Chemical structures of felodipine (FEL) and HPMCAS.

5.2.2. Methods

5.2.2.1. Preparation of physical mixtures and solid dispersions by rotary evaporation

Initial pretests of varying drug loads suggested that 50% FEL in polymer was rather challenging for amorphous stability, which therefore provided a suitable reference concentration in the ASDs of the main study. Binary mixtures of 50% w/w FEL polymer were

then prepared by dissolving drug and polymer in a solvent mixture of 50:50 (v/v) di-chloromethane: methanol. All solvent mixtures were visually inspected to confirm that the drug and the polymer were completely dissolved, and the systems formed uniform one-phase solutions. The solvent was then removed at 50 °C under reduced pressure using a rotavapor RE120 (Bünchi Labortechnik AG, Flawil, Switzerland) with a vacuum controller CVC2 (Vacuubrand GMBH+CO, Wertheim, Germany). The obtained solid mass was stored at room temperature overnight to re- move any residual solvents. The ASDs were freeze/milled with SPEX SamplePrep model 6770 (Metuchen, New jersey, USA). For a comparison with amorphous formulations, physical mixtures (PM) were pre- pared by mixing the powders of FEL and polymer for 5 min with a spatula.

Samples of the solid dispersions were compressed to tablets for subsequent surface and image analysis. Thus, powders (100 mg) were manually fed into a hydraulic XP1 press (Korsch AG, Berlin, Germany) and manually compacted. The compacts were flat-faced and round with a diameter of 7 mm.

5.2.2.2. X-ray powder diffraction

X-ray powder diffractogram (XRPD) were determined for PM as well as for ASD obtained from rota-evaporation. A D2 Phaser diffractometer (Bruker AXS GmbH, Karlsruhe, Germany) was employed that was equipped with a Co-2K KFL diffraction tube configured and a 1D- Lynxeye detector and with a Fe filter. The applied voltage and current were 30 kV and 10 mA, respectively. Diffraction patterns were obtained using a step width of 0.02° with a detector resolution in 2θ between 6 and 40° and a scan speed of 2 s/step at room temperature.

5.2.2.3. Stability studies

Compacts were stored in hermetically closed glass vials at a temperature of 40 °C using a climate chamber (Binder GmnH, Tuttlingen, Germany). The storage temperature was selected as a realistic but accelerating condition to detect kinetic changes over time (e.g. phase separation and/or drug crystallization). Samples were taken at specific time intervals and analyzed physically.

5.2.2.4. Scanning electron microscopy and energy-dispersive X-ray spectroscopy

The samples were placed on double-sided adhesive carbon tabs and the surface of the compacts was coated with gold under argon vacuum with a Sputter Coater SC7620 (Quorum Technologies Ltd., Kent, UK). These surfaces were then studied by means of scanning electron microscopy (SEM) TM3030 PLUS (Hitachi High-Technologies Corporation, Tokyo, Japan) and micrographs were collected in a mix mode. The microscope was equipped with an energy-dispersive X-ray spectroscopy (EDS) device for elemental mapping. The analysis was based on a Quantax 70 system software (Bruker Nano GmbH, Berlin, Germany) consisting of an X Flash Min SVE signal processing unit, a scan generator and Megalink interface together with an X Flash silicon drift detector 410/30H (Bruker Nano GmbH, Berlin, Germany). Samples were scanned during 300 s at a voltage of 15 kV to map the drug distribution of chloride (Cl) atoms for comparatively higher X-ray scattering intensity. This procedure was performed on all compacts at random location in spot sizes of 113×85 µm2.

5.2.2.5. 3D-Laser scanning confocal microscopy

Laser scanning micrographs of the sample surfaces were collected by means of a 3D laser scanning confocal microscopy (LSM) VK-X200 (Keyence, Osaka, Japan) using a violet laser (408 nm) and a 150x objective lens (Nikon Plan CF Apo, 150x/0.95, WD 0.2 mm). The surface is scanned at high speed in X, Y and Z, allowing image capturing and height measurements with high lateral resolution. Reflected white light and laser light emitted from the focal point are reflected back through the objective lens. The intensity of the laser light that passes through a pinhole is determined by a very sensitive 16-bit photomultiplier. Since the pinhole blocks most of the returning light (except the light from the focal point), confocal LSM delivers much sharper images than conventional microscopy techniques. In addition, a true color image from the integrated second light source is overlaid.

5.2.2.6. Atomic force microscopy

Atomic force microscopy (AFM) images of compacts were acquired at ambient conditions in dynamic AC mode using a NanoWizard 4 AFM instrument (JPK Instruments AG, Berlin, Germany). Height and phase images were collected simultaneously using a silicon PPP-NCHR cantilever (Nanosensors AG, Neuchâtel, Switzerland) with a resonance frequency of approximately 320 kHz and 42 Nm^{-1} spring constants.

5.2.2.7. Image processing

The Cl distribution images were exported to Image J software (National Institutes of Health, Bethesda, Maryland, USA) and converted to maximum intensity projection. In a second step, the gray scale images in the bmp format (with 1023×766 pixels and a resolution 72 dpi) were resized to the png format with 512×512 pixels while keeping the same resolution. The projected images were unsharpened with a radius of 12 pixels and they were binarized using MATLAB software package, version R2017b (The MathWorks, Inc., Natick, USA). In a binary image, a signal pixel is defined as a digital element whose intensity is 1 after thresholding the images of 5 and this conversion to binary format (with a resolution of 96 dpi) was conducted with 10 images per each sample analysis.

5.2.2.8. Multifractal and statistical data analysis

While classical fractals are mathematical objects with a single fractal dimension, multifractal formalism decomposes self-similar measures into intertwined fractal sets [41]. A brief review of basic multifractal theory is given in the Appendix.

Box-counting method algorithm was used to cover a 2-D image for determination of fractal dimensions. Using the binary images, boxes (grids of 512 pixel sizes) were counted using at least one pixel of the observed object. A multifractal spectrum was then determined with a customized MATLAB program as proposed and described previously [41].

The formalism of multifractals expresses here a generalized fractal dimension or a "deformation parameter" of variability degrees (Dq) and moment order (q) that is a number within $[-\infty; +\infty]$ interval extracting characteristics of the cluster distribution [39]. The multifractal spectra or the generalized dimension can be restricted to three values of particular interest D_0, D_1 and D_2. Herein, D_0 is the "classical box- counting dimension" also called the "capacity" dimension and D_1 refers to an information dimension (related to Shannon's measure of entropy) and characterizes the degree of disorder in a distribution. Finally, D_2 is named a "correlation" dimension so it indirectly marks a degree of clustering [40] [41][43].

The obtained fractal dimensions at the different time points were compared statistically by means of an analysis of the variance (ANOVA). STATGRAPHICS Centurion XVI ed. Professional (V. 16.1.15) from Statpoint Technologies Inc. (Warranton, Virginia, USA) was

used for all statistical calculations and a p-value < 0.05 was considered as significant. For comparison of the means, Fisher's procedure of the least significant difference (LSD) was calculated for 95% confidence intervals.

5.3. Results

5.3.1. Physical characterization

XRPD is a standard method to detect crystalline material based on distinct peaks arising from Bragg scattering from defined crystal planes. The absence of diffraction peaks in the initial analysis of solid dispersions were therefore an indicator of successful amorphization of FEL at a comparatively high load of 50% (w/w). A subsequent storage during four weeks at 40 °C did also not lead to samples in which crystalline drug was evidenced so the formulations were still unchanged at least based on XRPD (Fig. 11). By contrast, the analysis following eight weeks of storage (40 °C) revealed diffraction peaks of FEL, which was an obvious consequence of re-crystallization from the amorphous solid state. The diffraction peaks in the LF grade appeared to be more pronounced than in case of HF.
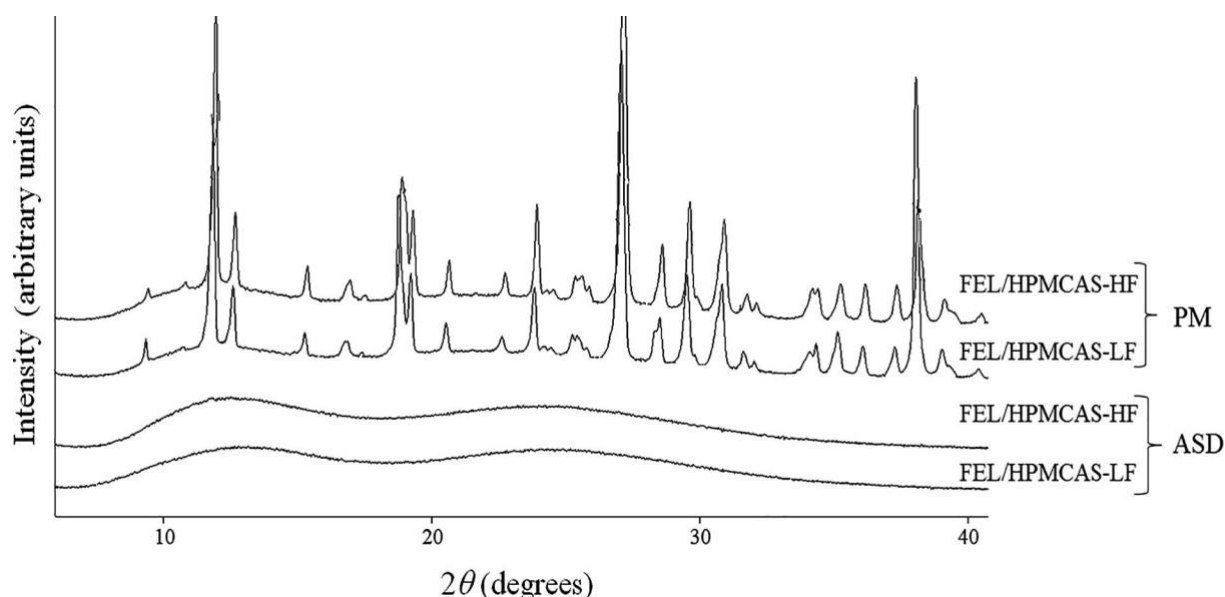
Fig. 11. Powder X-ray diffraction of FEL in physical mixture (PM) with HPMCAS of different polymer grades and formulated as amorphous solid dispersion (ASD). From bottom to top: ASDs: FEL/HPMCAS-LF, FEL/HPMCAS-HF after 4 weeks stored at 40 °C; PM: FEL/HPMCAS-LF, FEL/HPMCAS-HF (all samples at a drug load of 50 wt% of FEL).

5.3.2. Scanning electron microscopy and energy-dispersive X-ray spectroscopy

A suitable way to analyze the chemical distribution of specific atoms (as markers of molecules) on a surface is facilitated by SEM-EDS mapping. It is a qualitative method of chemical imaging and in this study, chloride was studied as characteristic marker of FEL since this was the only Cl-containing component in the formulation. The SEM-EDS binary micrographs of surface topography are presented in Fig. 12. Images of freshly prepared formulations and of those that show rearrangements of clusters over time (at 40 °C) are shown. The white pixels hold for the chloride (and hence FEL) distribution and it is possible to see some changes in the degree of clustering. However, only qualitative changes are detectable to a limited extent by the naked eye so that a more quantitative analysis is required to study cluster dynamics for which the multifractal formalism is applied.
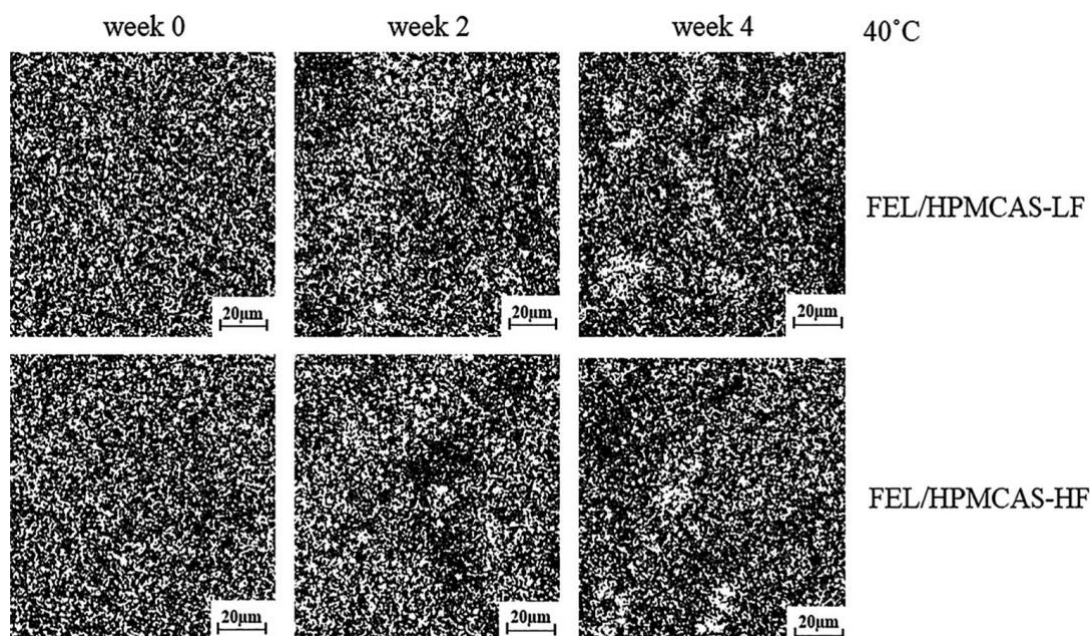
Fig. 12. Results of energy dispersive X-ray spectroscopy (EDS) to obtain two-dimensional binary images of ASDs FEL/HPMCAS-LF, FEL/HPMCAS-HF (50 wt% of FEL), following storage at 40 °C. Drug-rich phase is shown as white domains.

5.3.3. Multifractal analysis

Table 4 shows the results of multifractal analysis in terms of the dimensions with q values from zero to two. The different D_q values were pointing to multifractals as a better model than to assume a simpler monofractal cluster distribution, which would entail a constant D_q. This was even more clearly seen when dimensions at any time point were plotted for a broader range

of q values, as a typical sigmoidal shape was evidenced with decreasing Dq along decreasing q values (not shown).

Table 4

Generalized fractal dimensions of felodipine (FEL) solid dispersions over time as based on chemical imaging and conversion to binary pictures.

	Age (weeks)	Generalized fractal dimensions		
		$D0$	$D1$	$D2$
FEL/HPMCAS-LF	0	1.92 ± 0.01	1.88 ± 0.01	1.81 ± 0.02
(50:50)	2	1.92 ± 0.01	1.88 ± 0.01	1.81 ± 0.02
	4	1.91 ± 0.01	1.86 ± 0.01	1.79 ± 0.01
FEL/HPMCAS-HF	0	1.93 ± 0.00	1.89 ± 0.00	1.82 ± 0.01
(50:50)	2	1.92 ± 0.01	1.88 ± 0.01	1.81 ± 0.02
	4	1.91 ± 0.01	1.87 ± 0.02	1.80 ± 0.02

The capacity dimension D$_0$ was clearly below two for the Euclidian dimension but still comparatively high suggesting rather dense fractal structures. Values for D$_1$ and D$_2$ were also in a similar range as compared to our previous study [25]. The changes over time were focused on the early stage of stability testing, which did not reveal recrystallization based on classical XRPD testing. However, Table 4 indicates some changes of D$_q$ over time, which were statistically analyzed. An analysis of the variance (ANOVA) was conducted with time and polymer grade as factors and the generalized fractal dimensions (D$_0$, D$_1$, and D$_2$) were indeed found to be statistically significant to capture the microstructure changes, with significant p-values ($p < 0.0001$) for a time effect regarding any of the three dimensions studied. By contrast, the factor of HPMCAS grade was not found to be significant with respect to D$_0$, D$_1$, or D$_2$. Fig. 13 shows a statistical means plot together with Fisher's 95% LSD intervals. The significant storage effect was similar in extent for all fractal dimensions and is shown in Fig. 13 for D$_0$ as well as for D$_2$. The novel approach was obviously capable of identifying microstructural changes even in the early phase of stability testing.
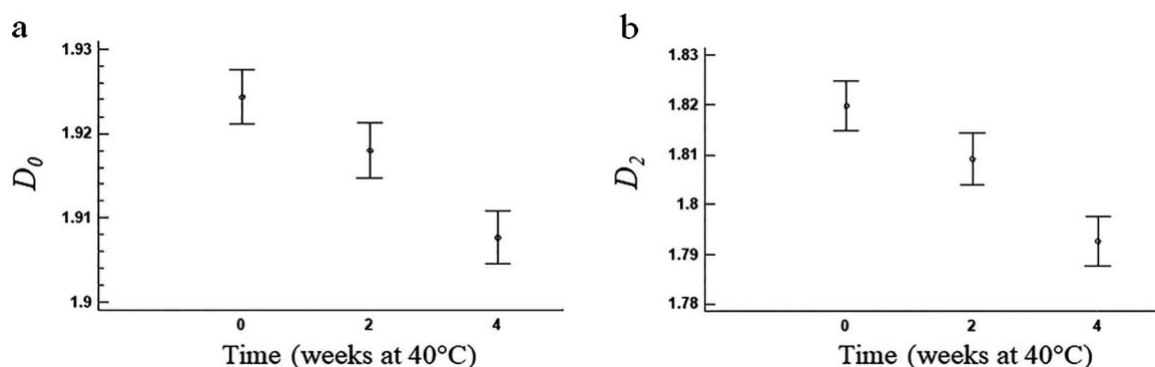
Fig. 13. Statistical means plot of FEL/HPMCAS ASD formulations (50 wt% of FEL) based on a two-factor ANOVA of how D0 (a) and D2 (b) are affected by storage time (at 40 °C), and intervals of Fisher's Least Significant Difference (LSD, 95%) are shown.

5.3.4. Laser scanning confocal microscopy

LSM provided nondestructive images in a relatively broad microstructural range for the different time points of early stability testing of FEL systems. Fig. 14 shows rather rough surfaces before storage (Fig. 14a/b) with hardly any crystals observed. Interestingly, the LSM images after 4 weeks (Fig. 14c/d) suggested generally smoother surfaces with some curved rough regions in the underlying microstructure for both formulations. Either for each system, a "blooming" effect was evidenced, which could be interpreted as crystals formed on top of the surface or protruding directly underneath the surface. Crystals and aggregations thereof were seen significantly in the system of FEL/HPMCAS-LF (Fig. 14c), but also from beneath and on top of the surface in the formulation of FEL/HPMCAS-HF (Fig. 14d). In general, LSM suggested occurrence of some crystals at early stability time (4 weeks, 40 °C).

5.3.5. Atomic force microscopy

Atomic force microscopy (AFM) is another physical surface analysis method that reaches small fields of view in a submicron range and is therefore complementary to LSM as a reference method of early stability testing.
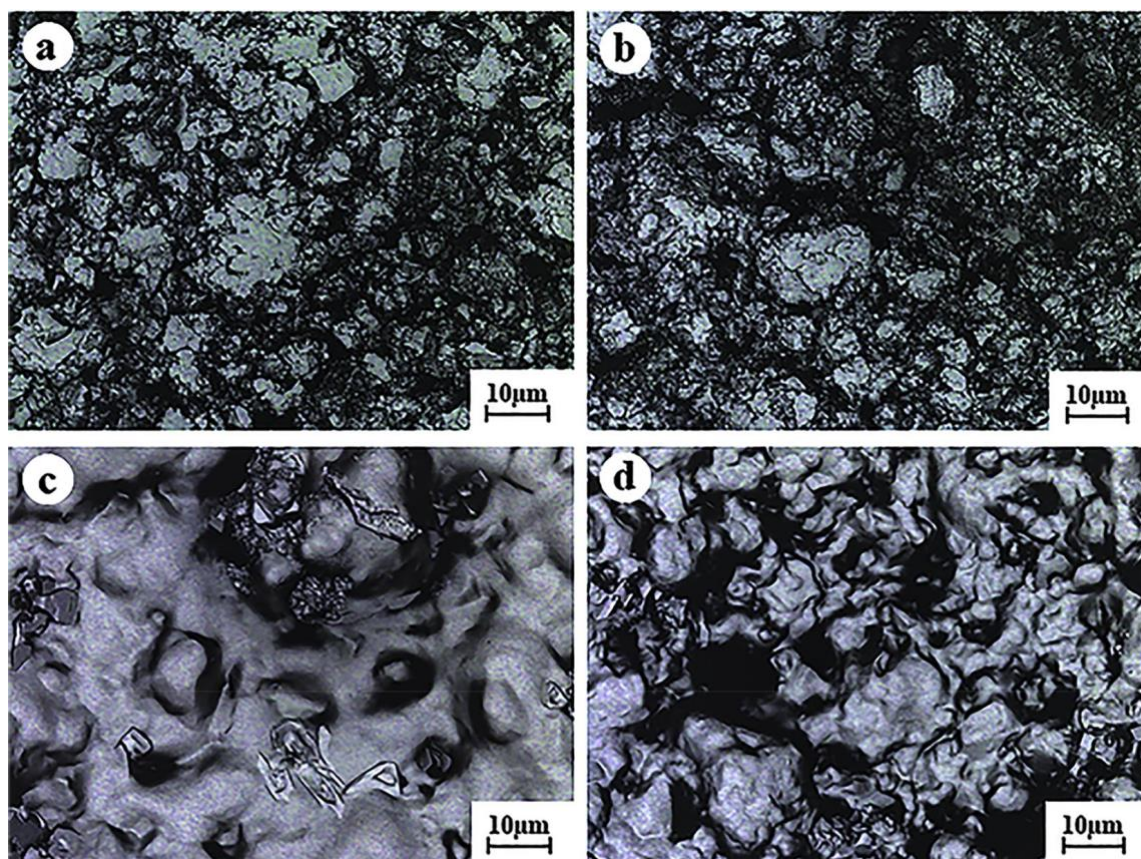
Fig. 14. Confocal laser microscopy of ASDs before storage (a, b) and after storage (c, d) for 4 weeks at 40 °C. FEL/HPMCAS-LF (a, c), FEL/HPMCAS-HF (b, d), at 50 wt % of FEL.

AFM topography (3D height) measurements were carried out to understand the morphology and growth dynamics of the surface before and after storage. The representative micrographs are visible in Fig. 15. The initial images show maximum height values of 100 nm (Fig. 15a) and 160 nm (Fig. 15b), respectively. Brighter islands or domain regions, most likely corresponding to FEL-rich domains surrounded by HPMCAS-rich domains, are indicated by peaks. The round edges of the FEL-rich domains indicate most likely that the aggregated clusters were still coated with polymer; therefore, minor phase contrast can be differentiated among these surfaces (Fig. 16a, b). These results are in line with previous literature [137]. AFM phase images were recorded to obtain a contrast due to variation in energy dissipation, which is related to the presence of differences in surface adherence and consequently different material properties. This technique also allows detecting localized variations in stiffness, so even more details of morphology can be obtained by phase contrast. Initial samples illustrate that the surfaces have a homogeneous contrast with brighter and darker regions co-existing

on the surface (Fig. 16a/b); hence material differences are less pronounced, assuming that the polymer is dominating and/or amorphous domains of the drug prevail upon crystal growth.
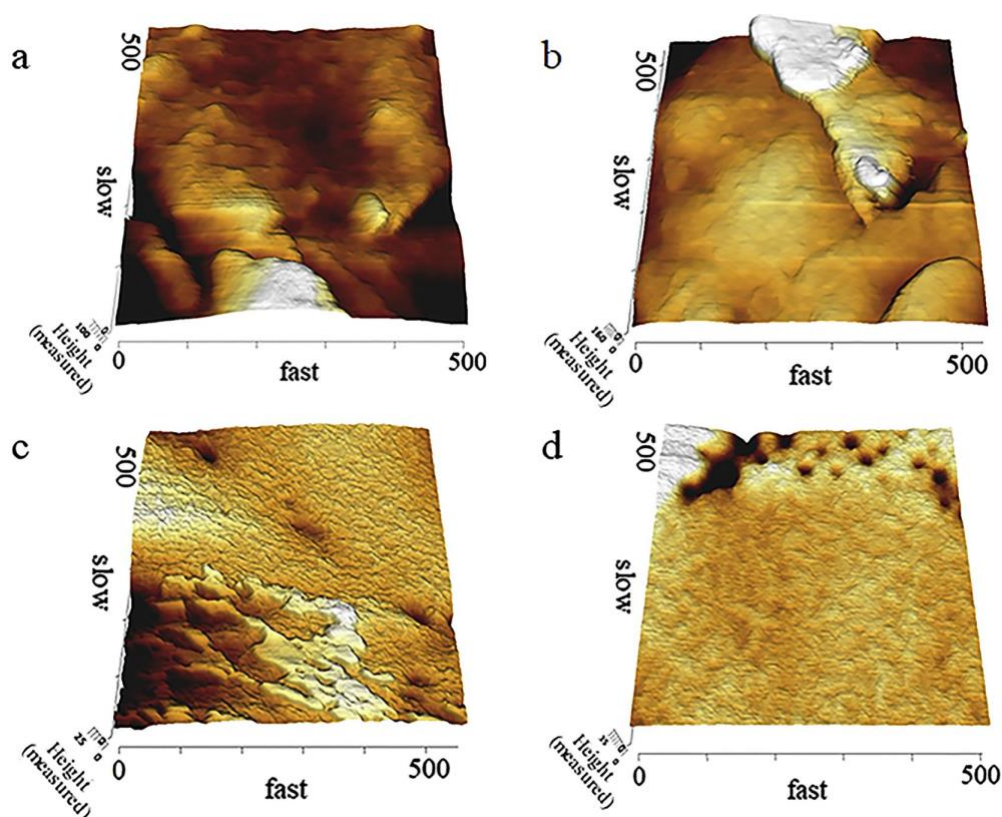
Fig. 16. AFM topographical images of FEL/HPMCAS ASDs before storage (a, b) and after storage (c, d) for 4 weeks at 40 °C. FEL/HPMCAS-LF (a, c) and FEL/HPMCAS-HF (b, d).
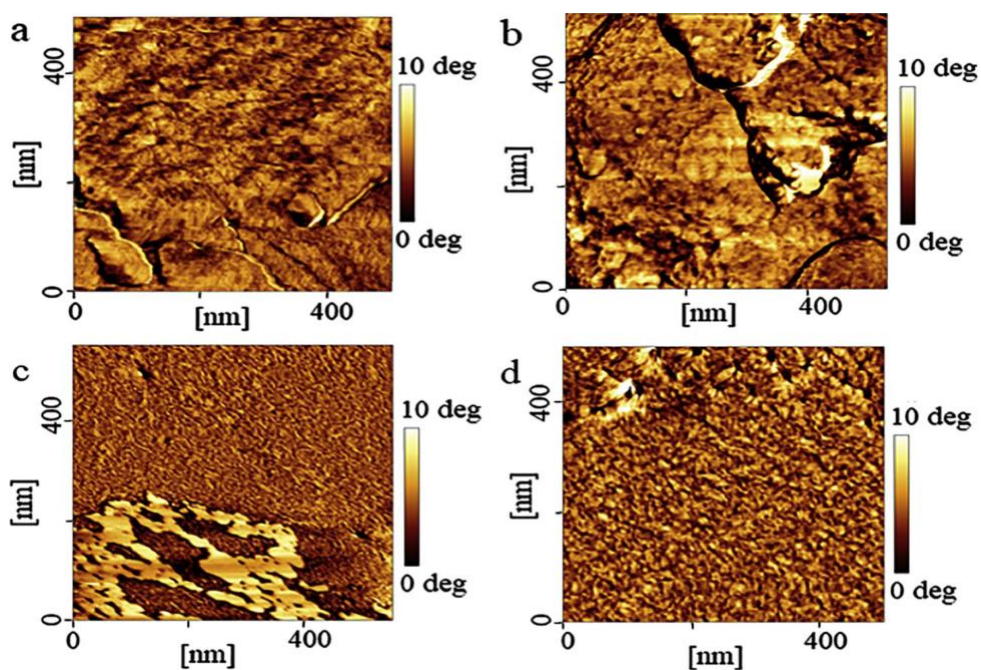
Fig. 16. AFM phase images of FEL/HPMCAS ASDs; before (a, b) and after storage (c, d) for 4 weeks at 40 °C. FEL/HPMCAS-LF (a, c) and FEL/HPMCAS-HF (b, d).

On the other hand, after storage at accelerated conditions for 4 weeks, the surface topography (Fig. 15c/d) shows a tendency to generally smoother (the height scale dropped to 14 nm and 30 nm, respectively), but more heterogeneous surfaces in the sense of growing phase separation as seen in the phase contrast images (Fig. 16c/d).

Both AFM modes (topography and phase imaging) strongly support each other and verify the obtained results giving a very detailed insight into the nanoscopic morphology of the specimen.

5.4. Discussion

The metastable character of ASD is a hurdle for their development because re-crystallization during long-term stability testing is a critical setback on the way to bring a drug product on the market. It is particularly critical when such physical instability is only detected late in pharmaceutical development, whereas an early identification of kinetically unstable formulations is less problematic in a screening phase. Accordingly, there is a tremendous interest in early identification of drug phase separation and re-crystallization from amorphous state. The present work is based on the hypothesis that multifractals can be helpful to early detect instability in amorphous drug formulations. The selected model systems showed some physical changes after four weeks with likely initial phase separation and occurrence of first crystals at the time of four weeks where XRPD still could not detect any changes. It was in line with expectation that LSM and AFM were more sensitive methods than XRPD to capture changes so these reference methods were interesting to compare with the novel multifractal approach based on SEM-EDS imaging.

As a result, differences in the multifractal dimensions D_0, D_1, and D_2 were indeed evidenced after one month compared to the initial analysis. Therefore, multifractals were capable of revealing microstructural changes caused by instability that were otherwise hard to identify from the original images of SEM-EDS and that were undetected by XRPD. Like any chemical imaging technique, SEM-EDS comes with spatial resolution limits and they impact on the determined clusters [139]. Such clusters hold for drug-rich domains and it is not possible to directly infer their physical state. These drug-rich regions can be of different kinds [133], e.g. concentrated drug associated with polymer or it can be separate amorphous drug domains considered in the binary images. Changes in these clusters are primarily changes in mathematical objects as captured by the fractal dimensions, D_0, D_1, and D_2. The physical

interpretation of these clusters should be always in the context of the applied imaging method. Since the multifractal dimensions provide meaning to cluster distributions, they can prove helpful for understanding any early changes in ASD as well as small crystal nuclei. This is important to keep in mind when clusters of drug are The dimension D_0 describes a space-filling capacity [105] and values decreased in the early period of stability testing. This result was not easy to predict because there are different possible processes like drug migration to the surface that may increase the space-filling capacity. An increase could also come from drug that was previously too dispersed and low concentrated to be detected as a drug-rich domain so that local aggregation can lead to new clusters. While these are processes to in- crease D_0, there are other effects leading to lowered values of this capacity dimension. Some of the drug-rich domains of drug-polymer aggregates may locally become more concentrated in an overall phase separation or drug re-crystallization. The resulting more concentrated clusters would appear still white in the binary images so that overall space coverage could slightly diminish.

The different cluster changes were apparently also leading on the average to a reduction in the information dimension D_1. This dimension reflects the diversity of elements in the system [42][78]. Moreover, D_2 holds for a correlation dimension [42][43][79] and the evidenced re- duction was caused by the microstructural changes. Thinking of the transformation from amorphous clusters to crystals there is of course nucleation as well as growth. Depending on which mechanism prevails, there would be different ways of how the correlation dimension changes. Thinking of the microstructural processes of phase separation, or crystal nucleation and growth, it is possible that different processes affect fractal dimensions in opposite directions, which could entail a loss of discrimination. The sensitivity to detect early physical instability by the multifractal approach is therefore certainly depending on the physical processes that occur as well as on the imaging technique used.

To compare the changes in cluster dynamics with other physical analysis methods, the sample surfaces were also studied by means of LSM and AFM. LSM and AFM are popular microscopic techniques to study surfaces with ultrahigh resolution [80][81]. While LSM can sample comparatively larger surfaces, AFM provides sub-micron images of surface topography and phase imaging.

The initial LSM micrograph profiles (Fig. 14a/b) of the surfaces were rather uneven and rough and both formulations had rather similar surface texture while hardly no crystals were seen. Compared to the initial rough micrographs, it is evident in Fig. 14c/d that there was a structural re-arrangement of the surface suggested likely caused by increased mobility [144].

The surfaces revealed in both formulations flat and smooth areas, and curved rough regions in the underlying micro- structure. It is suggested that after the storage at 40 °C, the temperature induced possible re-crystallization and aggregates of drug were formed, as can be observed, small groups of crystals with regular shape grow towards the surface as a result of re-crystallization.

Due to the small area of analysis, AFM was leading to an individual view on a sub-micron scale. The initial roughness is confirmed with a continuous matrix where critical spots of drug-rich domains might be occasionally recognized (Fig. 15a/b), while after storage the topography of the surfaces looked generally a bit smoother (Fig. 15c/d). From phase imaging, it is suggested that initially (Fig. 16a/b) the drug and the polymer were remaining both in the amorphous state and showed more or less homogenous contrast in the phase signal. The appearance of a brighter domain in the AFM phase image (Fig. 16c) gives evidence of the existence of crystalline domains among partially amorphous and highly dissipating polymer regions, indicating a heterogeneous surface due to the phase separation. These findings seem contradictory at first sight, but under the assumption that amorphous regions of the drug are re-crystallizing with accelerating temperature, the polymer needs to re- organize as well and starts to flatten out. This is in agreement with the relaxation phenomenon and mobility in glass state [18].

The orthogonal techniques LSM and AFM would be in line with the assumption that crystalline-amorphous phase separation may have occurred [133]. Based on this mechanism, a larger amount of drug can uniformly de-mix and segregate in a short amount of time, while nucleation and growth act only locally [145]. The de-mixing was likely to accelerate re-crystallization of drug.

In summary, the finding of the orthogonal methods of SEM-EDS, LSM and AFM suggest that even the freshly prepared solid dispersions had drug- rich and polymer-rich clusters and this heterogeneity was reflected in the binary images obtained from SEM-EDS. The subsequent dynamics of de mixing and re-crystallization was captured as complex changes in cluster dynamics of the binary images leading to measurable changes in multi- fractal dimension, LSM and AFM images, whereas in the classical XRPD analysis no changes were observed throughout the same time period.

5.5. Conclusions

The present work addressed the need for novel tools in early identification of physical instability of solid dispersions. Multifractal analysis was introduced successfully to early stages of stability testing using amorphous solid dispersions. Changes in the fractal dimensions were noted early in stability testing, when no changes were appreciated based on XRPD analysis. The orthogonal techniques of SEM-EDS, LSM and AFM that are known to be sensitive for microstructural change, suggested that the initial solid dispersions already displayed heterogeneity in terms of drug-rich and polymer-rich domains and de- mixing of the components was likely to precede nucleation of crystal- line material.

A decrease of the fractal dimensions D_0, D_1 and D_2 was statistically significant after four weeks of stability testing, while a possible effect of the HPMCAS grade was not revealed. Although the use of multifractals was successful for early instability detection, care is needed to expect the same cluster dynamics in other solid dispersions too. We discussed that different mechanisms of microstructural change can affect clusters and therefore fractal dimensions. However, a clear strength of the presented data evaluation is that this cluster analysis can be based even on more than one physical method of imaging. It could be, for example, also used for imaging based on Raman or near infrared spectroscopy.

Moreover, it would be interesting to study different types of solid dispersions. The present work holds much promise, but further research is needed to better assess the capability of multifractals to act as early warning tool for physical changes in metastable drug formulations.

Appendix A

Multifractal theory

The fractal dimension is measured by overlaying the binary image with grid of boxes and counting the number of boxes, $N(\varepsilon)$, this is expressed as [40][41]

$$N(\varepsilon) \sim \varepsilon^{-D_0} \tag{1}$$

where D_0 is the fractal dimension, calculated from the following equation:

$$D_0 = \lim_{\varepsilon \to 0} \frac{\log N(\varepsilon)}{\log \frac{1}{\varepsilon}} \tag{2}$$

D_0 is derived by counting the number of boxes with various sizes to cover the image and then estimating the linear region in the log-log plot. However, complex structures may not entirely be described by single fractal dimension, but by multifractal analysis, which considers the amount of mass inside each box, in this way characterize these complex structures. The probability P_i of finding the object pixel in the ith box is determined by

$$P_i(\varepsilon) \sim \varepsilon^{\alpha_i} \tag{3}$$

where α_i is the singularity strength which corresponds to the density in the ith box.

The probability distribution for multifractal measurements is

$$\sum_i [Pi(\varepsilon)^q] \sim \varepsilon^{\tau(q)} \tag{4}$$

Where q is the exponent expressing the fractal properties in different scales of the object. τ(q) can be defined as:

$$\tau(q) = \lim_{r \to 0} [\ln(\sum_i P_i(\varepsilon)^q)]/\ln(1/\varepsilon) \tag{5}$$

The full plot of D_q versus q is representative of the strength of the multifractality of finite measure, and the generalized dimension D_q which is related with q can be expressed as

$$D_q = \tau(q) \Big/ (q - 1) \tag{6}$$

Also, the relationship between parameters of *f(α)* versus α are used to calculate the multifractal spectra:

$$N(\alpha) \sim \varepsilon^{-f(\alpha)} \tag{7}$$

where the number of boxes $N(\alpha)$ for each probability $P_i(\varepsilon)$ has singularity strengths between α and $\alpha + d\alpha$ is found to scale. $f(\alpha)$ against α, in general way it gives the "fractal dimension" $f(\alpha)$ of sets where the measure scales locally with the same exponent α. The multifractal spectrum gives one dimension for each set where the data scales similarly. The variable $f(\alpha(q))$ gives the local fractal dimension at resolution q. *f(α)* has the same information of generalized information D_q and can be defined as [39]–[41]:

$$f(\alpha(q)) = q\alpha(q) - \tau(q) \tag{8}$$

where α(q) can be defined as:

$$\alpha(q) = {}^{d\tau(q)}/_{dq} \qquad\qquad (9)$$

In case of monofractal, $D_0 = D_1 = D_2$, whereas different values $D_0 \geq D_1 \geq D_2$ indicate a multifractal system [39].

Chapter 6

Final remarks and outlook

Great strides have been made in formulation and process design of ASD. However, despite diverse successes and a wealth of generated information, there are further improvements that could be still made to accelerate development and enhance performance of ASDs. The present thesis focused on the application of fractal geometry to such solid dispersions. Thus, fractal dimensions were assigned to a heterogeneous structure that were observed from chemical imaging. The findings and insights into the microstructure enabled a better process understanding and can help with decision making during formulation development.

Chemical imaging together with the multifractal approach proved to be reproducible and robust. This was suggested by the results obtained from microstructural imaging of different drug types and varying concentrations. The changes after the addition of an additive such as urea, showed clear effects on the different fractal dimensions. The study of the structural insights helped to better understand the performance of an ASD and may be used in the future also for another type of pharmaceutical dosage form. In this way the multifractal approach bears much promise from a theoretical as well as practical perspective.

This thesis also presents the need for novel tools in early identification of physical instability of solid dispersions. Multifractal analysis was introduced successfully to early stages of stability testing using ASD. Changes in the fractal dimensions were evidenced early in stability testing, when no changes were appreciated based on a comparative XRPD analysis. Although the use of multifractals was successful for early instability detection, care is needed to expect the same cluster dynamics in other solid dispersions too. We discussed that different

mechanisms of microstructural change can affect clusters and therefore fractal dimensions. However, a clear strength of the presented data evaluation is that this cluster analysis can be based even on more than one physical method of imaging.

It is also presented in this thesis that a microstructural study based on fractal geometry was helpful regarding the method selection for preparation of ASD. The influence was investigated by comparing different manufacturing techniques, such as: solvent coprecipitation, solvent evaporation and fusion method, while keeping the same drug loading. It was concluded that the fusion method was the best manufacturing technique for the systems studied, proving the importance of heating for this model system. The multifractal approach provided an effective characterization of the microstructure obtained from the different manufacturing technologies.

In general, this thesis presents an effective data evaluation approach based on imaging to obtain structural insights from ASDs. The different applications from early stability testing to study of microstructural differences cause by excipients, drug load and processes appear to be highly attractive from a development as well as manufacturing viewpoint. Therefore, the multifractal approach bears a strong potential to improve microstructural understanding, which is beneficial especially in Quality by Design framework and can be harnessed in the future also for other dosage forms and other underlying imaging techniques than used in this study.

Bibliography

[1]   S. Baghel, H. Cathcart, and N. J. O'Reilly, "Polymeric Amorphous Solid Dispersions: A Review of Amorphization, Crystallization, Stabilization, Solid-State Characterization, and Aqueous Solubilization of Biopharmaceutical Classification System Class II Drugs," *J. Pharm. Sci.*, vol. 105, no. 9, pp. 2527–2544, 2016.

[2]   S. A. Devi, K. Vasundhara, and S. Meraj Sultana, "A review on solid disperesions," *World J. Pharm. Res.*, vol. 7, no. 07, pp. 665–692, 2018.

[3]   S. Huang and R. O. Williams, "Effects of the Preparation Process on the Properties of Amorphous Solid Dispersions," *AAPS PharmSciTech*, no. 12, 2017.

[4]   G. Van Den Mooter, "The use of amorphous solid dispersions: A formulation strategy to overcome poor solubility and dissolution rate," *Drug Discov. Today Technol.*, vol. 9, no. 2, pp. e79–e85, 2012.

[5]   A. Haser and F. Zhang, "New Strategies for Improving the Development and Performance of Amorphous Solid Dispersions," *AAPS PharmSciTech*, vol. 19, no. 3, pp. 978–990, 2018.

[6]   C. Leuner and J. Dressman, "Improving drug solubility for oral delivery using solid dispersions," *Eur. J. Pharm. Biopharm.*, vol. 50, no. 1, pp. 47–60, 2000.

[7]   Y. Huang and W.-G. Dai, "Fundamental aspects of solid dispersion technology for poorly soluble drugs," *Acta Pharm. Sin. B*, vol. 4, no. 1, pp. 18–25, 2014.

[8]   T. Van Duong and G. Van den Mooter, "The role of the carrier in the formulation of pharmaceutical solid dispersions. Part II: amorphous," *Expert Opin. Drug Deliv.*, vol. 13, no. 12, pp. 1681–1694, 2016.

[9]   A. Newman, G. Knipp, and G. Zografi, "Assessing the Performance of Amorphous Solid Dispersions," *IJOURNAL Pharm. Sci.*, vol. 101, no. 4, pp. 1355–1377, 2012.

[10]   A. Paudel, M. Geppi, and G. Van Den Mooter, "Structural and dynamic properties of amorphous solid dispersions: The role of solid-state nuclear magnetic resonance spectroscopy and relaxometry," *J. Pharm. Sci.*, vol. 103, no. 9, pp. 2635–2662, 2014.

[11]   G. Zografi and A. Newman, "Interrelationships Between Structure and the Properties of

Amorphous Solids of Pharmaceutical Interest," *J. Pharm. Sci.*, vol. 106, no. 1, pp. 5–27, 2017.

[12] E. O. Kissi, H. Grohganz, K. Löbmann, M. T. Ruggiero, J. A. Zeitler, and T. Rades, "Glass-Transition Temperature of the β-Relaxation as the Major Predictive Parameter for Recrystallization of Neat Amorphous Drugs," *J. Phys. Chem. B*, p. acs.jpcb.7b10105, 2018.

[13] J. Sibik and J. A. Zeitler, "Direct measurement of molecular mobility and crystallisation of amorphous pharmaceuticals using terahertz spectroscopy," *Adv. Drug Deliv. Rev.*, vol. 100, pp. 147–157, 2016.

[14] P. Mistry, K. K. Amponsah-Efah, and R. Suryanarayanan, "Rapid Assessment of the Physical Stability of Amorphous Solid Dispersions," *Cryst. Growth Des.*, vol. 17, no. 5, pp. 2478–2485, 2017.

[15] C. Correa-Soto *et al.*, "Second harmonic generation microscopy as a tool for the early detection of crystallization in spray dried dispersions," *J. Pharm. Biomed. Anal.*, vol. 146, pp. 86–95, 2017.

[16] N. K. Thakral, S. Mohapatra, G. A. Stephenson, and R. Suryanarayanan, "Compression-induced crystallization of amorphous indomethacin in tablets: Characterization of spatial heterogeneity by two-dimensional X-ray diffractometry," *Mol. Pharm.*, vol. 12, no. 1, pp. 253–263, 2015.

[17] N. Li, C. J. Gilpin, and L. S. Taylor, "Understanding the Impact of Water on the Miscibility and Microstructure of Amorphous Solid Dispersions: An AFM-LCR and TEM-EDX Study," *Mol. Pharm.*, vol. 14, no. 5, pp. 1691–1705, 2017.

[18] M. Descamps and E. Dudognon, "Crystallization from the amorphous state: Nucleation-growth decoupling, polymorphism interplay, and the role of interfaces," *J. Pharm. Sci.*, vol. 103, no. 9, pp. 2615–2628, 2014.

[19] P. Y. Sacré *et al.*, "A new criterion to assess distributional homogeneity in hyperspectral images of solid pharmaceutical dosage forms," *Anal. Chim. Acta*, vol. 818, pp. 7–14, 2014.

[20] M. L. Scherholz, B. Wan, and G. Mcgeorge, "Research Article A Rational Analysis of Uniformity Risk for Agglomerated Drug Substance Using NIR Chemical Imaging," *AAPS PharmSciTech*, 2016.

[21]   N. L. Calvo, R. M. Maggio, and T. S. Kaufman, "Characterization of pharmaceutically relevant materials at the solid state employing chemometrics methods," *J. Pharm. Biomed. Anal.*, vol. 147, pp. 538–564, 2018.

[22]   B. Vajna, H. Pataki, Z. Nagy, I. Farkas, and G. Marosi, "Characterization of melt extruded and conventional Isoptin formulations using Raman chemical imaging and chemometrics," *Int. J. Pharm.*, vol. 419, no. 1–2, pp. 107–113, 2011.

[23]   S. Rades *et al.*, "High-resolution imaging with SEM/T-SEM, EDX and SAM as a combined methodical approach for morphological and elemental analyses of single engineered nanoparticles," *RSC Adv.*, vol. 4, no. 91, pp. 49577–49587, 2014.

[24]   N. Scoutaris, K. Vithani, I. Slipper, B. Chowdhry, and D. Douroumis, "SEM/EDX and confocal Raman microscopy as complementary tools for the characterization of pharmaceutical tablets," *Int. J. Pharm.*, vol. 470, no. 1–2, pp. 88–98, 2014.

[25]   S. Hellstén, H. Qu, T. Heikkilä, J. Kohonen, S.-P. Reinikainen, and M. Louhi-Kultanen, "Raman spectroscopic imaging of indomethacin loaded in porous silica," *CrystEngComm*, vol. 14, no. 5, pp. 1582–1587, 2012.

[26]   H. Ueda, Y. Ida, K. Kadota, and Y. Tozuka, "Raman mapping for kinetic analysis of crystallization of amorphous drug based on distributional images," *Int. J. Pharm.*, vol. 462, no. 1–2, pp. 115–122, 2014.

[27]   L. Bao, J. Ma, W. Long, P. He, T. A. Zhang, and A. V. Nguyen, "Fractal analysis in particle dissolution: A review," *Rev. Chem. Eng.*, vol. 30, no. 3, pp. 261–287, 2014.

[28]   C. Demetzos and N. Pippa, "Fractal analysis as a complementary approach to predict the stability of drug delivery nano systems in aqueous and biological media: A regulatory proposal or a dream?," *Int. J. Pharm.*, vol. 473, no. 1–2, pp. 213–218, 2014.

[29]   N. Ruschin-Rimini, I. Ben-Gal, and O. Maimon, "Fractal geometry statistical process control for non-linear pattern-based processes," *IIE Trans. (Institute Ind. Eng.*, vol. 45, no. 4, pp. 355–373, 2013.

[30]   Z. Jelcic, K. Hauschild, M. Ogiermann, and K. M. Picker-Freyer, "Evaluation of tablet formation of different lactoses by 3D modeling and fractal analysis," *Drug Dev. Ind. Pharm.*, vol. 33, no. 4, pp. 353–372, 2007.

[31]   X. Zhang, Y. Xu, and R. L. Jackson, "An analysis of generated fractal and measured rough surfaces," *Electr. Contacts, Proc. Annu. Holm Conf. Electr. Contacts*, vol. 2016–

Decem, no. June 2016, pp. 192–197, 2016.

[32]   Z. Chen, Y. Liu, and P. Zhou, "A comparative study of fractal dimension calculation methods for rough surface profiles," *Chaos, Solitons and Fractals*, vol. 112, pp. 24–30, 2018.

[33]   P. D. Domański and M. Ławryńczuk, "Assessment of predictive control performance using fractal measures," *Nonlinear Dyn.*, vol. 89, no. 2, pp. 773–790, 2017.

[34]   D. Z. Chen *et al.*, "Fractal atomic-level percolation in metallic glasses," *Science (80-.).*, vol. 349, no. 6254, pp. 1306–1310, 2015.

[35]   N. Pippa, A. Dokoumetzidis, C. Demetzos, and P. Macheras, "On the ubiquitous presence of fractals and fractal concepts in pharmaceutical sciences: A review," *Int. J. Pharm.*, vol. 456, no. 2, pp. 340–352, 2013.

[36]   C. Adler, A. Teleki, and M. Kuentz, "Multifractal Characterization of Pharmaceutical Hot-Melt Extrudates," *Pharm. Res.*, vol. 34, no. 2, pp. 321–332, 2017.

[37]   X. Yin *et al.*, "Fractal structure determines controlled release kinetics of monolithic osmotic pump tablets," *J. Pharm. Pharmacol.*, vol. 65, no. 7, pp. 953–959, 2013.

[38]   V. Blavatska and W. Janke, "Multifractality of self-avoiding walks on percolation clusters," *Phys. Rev. Lett.*, vol. 101, no. 12, pp. 1–4, 2008.

[39]   H. Salat, R. Murcio, and E. Arcaute, "Multifractal methodology," *Physica A*, vol. 473, pp. 467–487, 2017.

[40]   K. Liu and M. Ostadhassan, "Quantification of the microstructures of Bakken shale reservoirs using multi-fractal and lacunarity analysis," *J. Nat. Gas Sci. Eng.*, vol. 39, pp. 62–71, 2017.

[41]   D. J. Gould, T. J. Vadakkan, R. A. Poché, and Dj. M. E. Dickinson, "Multifractal and Lacunarity Analysis of Microvascular Morphology and Remodeling," pp. 136–151, 2011.

[42]   A. Giri, S. Tarafdar, P. Gouze, and T. Dutta, "Multifractal analysis of the pore space of real and simulated sedimentary rocks," *Geophys. J. Int.*, vol. 200, no. 2, pp. 1106–1115, 2015.

[43]   T. Kano, Y. Yoshihashi, E. Yonemochi, and K. Terada, "Clarifying the mechanism of aggregation of particles in high-shear granulation based on their surface properties by

using micro-spectroscopy," *Int. J. Pharm.*, vol. 461, no. 1–2, pp. 495–504, 2014.

[44]   Ž. Mitić *et al.*, "Instrumental methods and techniques for structural and physicochemical characterization of biomaterials and bone tissue: A review," *Mater. Sci. Eng. C*, vol. 79, pp. 930–949, 2017.

[45]   N. Shah, H. Sandhu, D. S. Choi, H. Chokshi, and A. W. Malick, *Amorphous Solid Dispersion - Theory and Practice*. 2014.

[46]   S. Dedroog, C. Huygens, and G. Van den Mooter, "Chemically identical but physically different: a comparison of spray drying, hot melt extrusion and cryo-milling for the formulation of high drug loaded amorphous solid dispersions of naproxen," *Eur. J. Pharm. Biopharm.*, vol. 135, no. September 2018, pp. 1–12, 2018.

[47]   A. Newman, D. Engers, S. Bates, I. Ivanisevic, R. C. Kelly, and G. Zografi, "Characterization of Amorphous API:Polymer Mixtures Using X-Ray Powder Diffraction," *J. Pharm. Sci.*, vol. 97, no. 11, pp. 4841–4856, 2008.

[48]   S. Laske *et al.*, "A Review of PAT Strategies in Secondary Solid Oral Dosage Manufacturing of Small Molecules," *J. Pharm. Sci.*, vol. 106, no. 3, pp. 667–712, 2017.

[49]   V. Mishra, S. Thakur, A. Patil, and A. Shukla, "Quality by design (QbD) approaches in current pharmaceutical set-up," *Expert Opin. Drug Deliv.*, vol. 15, no. 8, pp. 737–758, 2018.

[50]   C. C. Sun, "Microstructure of Tablet—Pharmaceutical Significance, Assessment, and Engineering," *Pharm. Res.*, vol. 34, no. 5, pp. 918–928, 2017.

[51]   T. Helešicová, T. Pekárek, and P. Matějka, "The influence of different acquisition settings and the focus adjustment on Raman spectral maps of pharmaceutical tablets," *J. Drug Deliv. Sci. Technol.*, vol. 47, no. July, pp. 386–394, 2018.

[52]   B. Kann and M. Windbergs, "Chemical Imaging of Drug Delivery Systems with Structured Surfaces–a Combined Analytical Approach of Confocal Raman Microscopy and Optical Profilometry," *AAPS J.*, vol. 15, no. 2, pp. 505–510, 2013.

[53]   R. Abreu-Villela, M. Schönenberger, I. Caraballo, and M. Kuentz, "Early stages of drug crystallization from amorphous solid dispersion via fractal analysis based on chemical imaging," *Eur. J. Pharm. Biopharm.*, vol. 133, no. September, pp. 122–130, 2018.

[54]   J. F. Gamble, M. Tobyn, and R. Hamey, "Application of image-based particle size and

shape characterization systems in the development of small molecule pharmaceuticals," *J. Pharm. Sci.*, vol. 104, no. 5, pp. 1563–1574, 2015.

[55] K. Lundstedt-Enkel *et al.*, "Different multivariate approaches to material discovery, process development, PAT and environmental process monitoring," *Chemom. Intell. Lab. Syst.*, vol. 84, no. 1–2 SPEC. ISS., pp. 201–207, 2006.

[56] Á. Aguilar-de-Leyva, M. D. Campiñez, M. Casas, and I. Caraballo, "Design space and critical points in solid dosage forms," *J. Drug Deliv. Sci. Technol.*, vol. 42, pp. 134–143, 2017.

[57] K. Patwardhan, F. Asgarzadeh, T. Dassinger, J. Albers, and M. A. Repka, "A quality by design approach to understand formulation and process variability in pharmaceutical melt extrusion processes," *J. Pharm. Pharmacol.*, vol. 67, no. 5, pp. 673–684, 2015.

[58] L. X. Yu *et al.*, "Understanding Pharmaceutical Quality by Design," *AAPS J.*, vol. 16, no. 4, pp. 771–783, 2014.

[59] T. J. N. Watson, R. Nosal, J. Lepore, and F. Montgomery, "Misunderstanding Design Space : a Robust Drug Product Control Strategy Is the Key to Quality Assurance," *J. Pharm. Innov.*, vol. 13, no. 3, pp. 10–12, 2018.

[60] R. G. Brereton *et al.*, "Chemometrics in analytical chemistry—part I: history, experimental design and data analysis tools," *Anal. Bioanal. Chem.*, vol. 409, no. 25, pp. 5891–5899, 2017.

[61] N. Willecke, A. Szepes, M. Wunderlich, J. P. Remon, C. Vervaet, and T. De Beer, "A novel approach to support formulation design on twin screw wet granulation technology: Understanding the impact of overarching excipient properties on drug product quality attributes," *Int. J. Pharm.*, vol. 545, no. 1–2, pp. 128–143, 2018.

[62] S. D. Stamatis and L. E. Kirsch, "Using Manufacturing Design Space Concepts for Stability Risk Assessment—Gabapentin NIPTE/FDA Case Study," *AAPS PharmSciTech*, vol. 19, no. 7, pp. 2801–2807, 2018.

[63] S. Dai *et al.*, "SeDeM expert system for directly compressed tablet formulation: A review and new perspectives," *Powder Technol.*, vol. 342, no. 11, pp. 517–527, 2019.

[64] I. Fuertes, I. Caraballo, A. Miranda, and M. Millán, "Study of critical points of drugs with different solubilities in hydrophilic matrices," *Int. J. Pharm.*, vol. 383, pp. 138–146, 2010.

[65] H. K. Janssen and O. Stenull, "Linear polymers in disordered media: The shortest, the longest, and the mean self-avoiding walk on percolation clusters," *Phys. Rev. E Stat. Nonlin. Soft Matter. Phys.*, vol. 85, no. 1, p. 011123, 2012.

[66] O. Stenull and H. K. Janssen, "Multifractal properties of resistor diode percolation," *Phys. Rev. E Stat. Nonlin. Soft Matter. Phys.*, vol. 65, no. 3, p. 036124, 2002.

[67] A. A. Saberi, "Recent advances in percolation theory and its applications," *Phys. Rep.*, vol. 578, pp. 1–32, 2015.

[68] S. Saremi and T. J. Sejnowski, "Correlated Percolation, Fractal Structures, and Scale-Invariant Distribution of Clusters in Natural Images," *IEEE Trans. Pattern Anal. Mach. Intell.*, vol. 38, no. 5, pp. 1016–1020, 2016.

[69] J. Liu and K. Regenauer-Lieb, "Application of percolation theory to microtomography of structured media: Percolation threshold, critical exponents, and upscaling," *Phys. Rev. E Stat. Nonlin. Soft Matter. Phys.*, vol. 83, no. 1, p. 016106, 2011.

[70] J. Ding, M. Asta, and R. O. Ritchie, "On the question of fractal packing structure in metallic glasses," *Proc. Natl. Acad. Sci.*, vol. 114, no. 32, pp. 8458–8463, 2017.

[71] S. P. Finner, M. I. Kotsev, M. A. Miller, and P. Van Der Schoot, "Continuum percolation of polydisperse rods in quadrupole fields: Theory and simulations," *J. Chem. Phys.*, vol. 148, no. 3, 2018.

[72] A. Coniglio, "Cluster structure near the percolation threshold," *J. Phys. A. Math. Gen.*, vol. 15, no. 12, p. 3829, 1982.

[73] M. Grassi and G. Grassi, "Application of mathematical modeling in sustained release delivery systems.," *Expert Opin. Drug Deliv.*, vol. 11, no. 8, pp. 1299–321, 2014.

[74] H. Leuenberger, R. Leu, and J. D. Bonny, "Application of percolation theory and fractal geometry to tablet compaction," *Drug Dev. Ind. Pharm.*, vol. 18, no. 6–7, pp. 723–766, 1992.

[75] Á. Aguilar-De-Leyva, T. Sharkawi, B. Bataille, G. Baylac, and I. Caraballo, "Release behaviour of clozapine matrix pellets based on percolation theory," *Int. J. Pharm.*, vol. 404, no. 1–2, pp. 133–141, 2011.

[76] I. Caraballo, "Factors affecting drug release from hydroxypropyl methylcellulose matrix systems in the light of classical and percolation theories," *Expert Opin. Drug Deliv.*, vol.

7, no. 11, pp. 1291–1301, 2010.

[77]   M. Casas, Á. Aguilar-de-leyva, and I. Caraballo, "Towards a rational basis for selection of excipients: Excipient Efficiency for controlled release," *Int. J. Pharm.*, vol. 494, no. 1, pp. 288–295, 2015.

[78]   R. Luginbühl and H. Leuenberger, "Use of percolation theory to interpret water uptake, disintegration time and intrinsic dissolution rate of tablets consisting of binary mixtures," *Pharm. Acta Helv.*, vol. 69, no. 3, pp. 127–134, 1994.

[79]   E. Krausbauer, M. Puchkov, G. Betz, and H. Leuenberger, "Rational Estimation of the Optimum Amount of Non-Fibrous Disintegrant Applying Percolation Theory for Binary Fast Disintegrating Formulation," *J. Pharm. Sci.*, vol. 95, no. 10, pp. 2145–2157, 2007.

[80]   T. Wenzel, C. Stillhart, P. Kleinebudde, and A. Szepes, "Influence of drug load on dissolution behavior of tablets containing a poorly water-soluble drug: estimation of the percolation threshold," *Drug Dev. Ind. Pharm.*, vol. 43, no. 8, pp. 1265–1275, 2017.

[81]   M. Kuentz and H. Leuenberger, "Modified Young's Modulus of Microcrystalline Cellulose Tablets and the Directed Continuum Percolation Model," *Pharm. Dev. Technol.*, vol. 3, no. 1, pp. 13–19, 1998.

[82]   M. Kuentz and H. Leuenberger, "Pressure Susceptibility of Polymer Tablets as a Critical Property : A Modified Heckel Equation," *J. Pharm. Sci.*, vol. 88, no. 2, pp. 174–179, 1999.

[83]   M. Kuentz, H. Leuenberger, and M. Kolb, "Fracture in disordered media and tensile strength of microcrystalline cellulose tablets at low relative densities," *Int. J. Pharm.*, vol. 182, pp. 243–255, 1999.

[84]   N. Ramírez, L. M. Melgoza, M. Kuentz, H. Sandoval, and I. Caraballo, "Comparison of different mathematical models for the tensile strength-relative density profiles of binary tablets," *Eur. J. Pharm. Sci.*, vol. 22, no. 1, pp. 19–23, 2004.

[85]   A. Kolesnikova, A. Zakinyan, and Y. Dikansky, "Microstructure formation and macroscopic dynamics of ferrofluid emulsion in rotating magnetic field," *EPJ Web Conf.*, vol. 185, p. 09004, 2018.

[86]   M. Draief, "Epidemic processes on complex networks: The effect of topology on the spread of epidemics," *Phys. A Stat. Mech. its Appl.*, vol. 363, no. 1, pp. 120–131, 2006.

[87] B. Yao, F. Imani, A. S. Sakpal, E. W. Reutze, and H. Yang, "Multifractal Analysis of Image Profiles for the Characterization and Detection of Defects in Additive Manufacturing," *J. Manuf. Sci. Eng*, vol. 140, no. 3, 2017.

[88] F. Imani, B. Yao, R. Chen, P. Rao, and H. Yang, "Fractal pattern recognition of image profiles for manufacturing process monitoring and control," *Int. Manuf. Sci. Eng. Conf.*, p. 1, 2018.

[89] W. Kirchmeyer, N. Wyttenbach, J. Alsenz, and M. Kuentz, "Influence of excipients on solvent-mediated hydrate formation of piroxicam studied by dynamic imaging and fractal analysis," *Cryst. Growth Des.*, vol. 15, no. 10, pp. 5002–5010, 2015.

[90] V. Shah and D. E. Booth, "A fractal dimension-based method for statistical process control," *Int. J. Oper. Res.*, vol. 14, no. 2, pp. 187–199, 2012.

[91] Y. Cho *et al.*, "Engineering the shape and structure of materials by fractal cut," *Proc. Natl. Acad. Sci.*, vol. 111, no. 49, pp. 17390–17395, 2014.

[92] M. A. Aon, B. O'Rourke, and S. Cortassa, "The fractal architecture of cytoplasmic organization: scaling, kinetics and emergence in metabolic networks.," *Mol. Cell. Biochem.*, vol. 256/257, no. 1–2, pp. 169–184, 2004.

[93] Z. Shireen and S. B. Babu, "Lattice animals in diffusion limited binary colloidal system," *J. Chem. Phys.*, vol. 147, no. 5, p. 054904, 2017.

[94] J. Esquena, C. Solans, and J. Llorens, "Nitrogen sorption studies of silica particles obtained in emulsion and microemulsion media," *J. Colloid Interface Sci.*, vol. 225, no. 2, pp. 291–298, 2000.

[95] K. Nidhi, S. Indrajeet, M. Khushboo, K. Gauri, and D. J. Sen, "Hydrotropy: A promising tool for solubility enhancement: A review," *Int. J. Drug Dev. Res.*, vol. 3, no. 2, pp. 26–33, 2011.

[96] B. P. Kolesnikov, "Influence of fractal substructures of the percolating cluster on transferring processes in macroscopically disordered environments," *J. Phys. Conf. Ser.*, vol. 891, no. 1, p. 012355, 2017.

[97] R. P. Wool, "Twinkling Fractal Theory of the Glass Transition," *J. Polym. Sci. Part B Polym. Phys.*, vol. 46, pp. 2765–2778, 2008.

[98] H. Leuenberger and M. Lanz, "Pharmaceutical powder technology - From art to science:

The challenge of the FDA's process analytical technology initiative," *Adv. Powder Technol.*, vol. 16, no. 1, pp. 3–25, 2005.

[99]   M. Leane *et al.*, "Manufacturing Classification System in the real world: factors influencing manufacturing process choices for filed commercial oral solid dosage formulations, case studies from industry and considerations for continuous processing," *Pharm. Dev. Technol.*, vol. 23, pp. 964–977, 2018.

[100]   M. Kuentz and H. Leuenberger, "A new theoretical approach to tablet strength of a binary mixture consisting of a well and a poorly compactable substance," *Eur. J. Pharm. Biopharm.*, vol. 49, pp. 151–159, 2000.

[101]   V. R. Nalluri and M. Kuentz, "Flowability characterisation of drug-excipient blends using a novel powder avalanching method," *Eur. J. Pharm. Biopharm.*, vol. 74, no. 2, pp. 388–396, 2010.

[102]   C. Hirschberg, J. P. Boetker, J. Rantanen, and M. Pein-Hackelbusch, "Using 3D Printing for Rapid Prototyping of Characterization Tools for Investigating Powder Blend Behavior," *AAPS PharmSciTech*, vol. 19, no. 2, pp. 941–950, 2017.

[103]   J. M. I. Alakoskela and P. K. J. Kinnunen, "Probing phospholipid main phase transition by fluorescence spectroscopy and a surface redox reaction," *J. Phys. Chem. B*, vol. 105, no. 45, pp. 11294–11301, 2001.

[104]   C. Demetzos and N. Pippa, "Fractal geometry as a new approach for proving nanosimilarity: A reflection note," *Int. J. Pharm.*, vol. 483, no. 1–2, pp. 1–5, 2015.

[105]   N. Pippa, S. Pispas, and C. Demetzos, "The fractal hologram and elucidation of the structure of liposomal carriers in aqueous and biological media," *Int. J. Pharm.*, vol. 430, no. 1–2, pp. 65–73, 2012.

[106]   M. Nematollahi, A. Jalali-Arani, and H. Modarress, "Effect of Nanoparticle Localization on the Rheology, Morphology and Toughness of Nanocomposites based on (Poly (Lactic Acid)/Natural Rubber/Nanosilica)," *Polym. Int.*, vol. 68, no. 4, pp. 779–787, 2019.

[107]   B. Guichard, P. Cassagnau, G. Sudre, R. Fulchiron, B. Ledieu, and E. Espuche, "Effect of a post-annealing process on microstructure and mechanical properties of high-density polyethylene/silica nanocomposites," *J. Polym. Sci. Part B Polym. Phys.*, pp. 1–12, 2019.

[108] E. V. White, D. Fullwood, K. M. Golden, and I. Zharov, "Percolation analysis for estimating the maximum size of particles passing through nanosphere membranes," *Phys. Rev. E*, vol. 99, no. 2, p. 022904, 2019.

[109] I. Caraballo, M. Millan, and A. M. Rabasco, "Relationship between drug percolation threshold and particle size in matrix tablets," *Pharmaceutical Research*, vol. 13, no. 3. pp. 387–390, 1996.

[110] I. Caraballo, M. Fernández-Arévalo, M. A. Holgado, and A. M. Rabasco, "Percolation theory: application to the study of the release behaviour from inert matrix systems," *Int. J. Pharm.*, vol. 96, no. 1–3, pp. 175–181, 1993.

[111] R. Abreu-Villela, C. Adler, I. Caraballo, and M. Kuentz, "Electron microscopy/energy dispersive X-ray spectroscopy of drug distribution in solid dispersions and interpretation by multifractal geometry," *J. Pharm. Biomed. Anal.*, vol. 150, pp. 241–247, 2018.

[112] C. Adler, A. Teleki, and M. Kuentz, "Multifractal and mechanical analysis of amorphous solid dispersions," *Int. J. Pharm.*, vol. 523, no. 1, pp. 91–101, 2017.

[113] J. BROUWERS, M. BREWSTER, and P. AUGUSTIJNS, "Supersaturating Drug Delivery Systems: The Answer to Solubility-Limited Oral Bioavailability?," *J. Pharm. Sci.*, vol. 98, no. 8, pp. 2549–2572, 2009.

[114] J. A. Baird and L. S. Taylor, "Evaluation of amorphous solid dispersion properties using thermal analysis techniques," *Adv. Drug Deliv. Rev.*, vol. 64, no. 5, pp. 396–421, 2012.

[115] N. Wyttenbach and M. Kuentz, "Glass-forming ability of compounds in marketed amorphous drug products," *Eur. J. Pharm. Biopharm.*, vol. 112, pp. 204–208, 2017.

[116] C. Adler, M. Schönenberger, A. Teleki, B. Leuenberger, and M. Kuentz, "Flow-through cross-polarized imaging as a new tool to overcome the analytical sensitivity challenges of a low-dose crystalline compound in a lipid matrix," *J. Pharm. Biomed. Anal.*, vol. 115, pp. 20–30, 2015.

[117] B. VAN EERDENBRUGH, M. LO, K. KJOLLER, C. MARCOTT, and L. TAYLOR, "Nanoscale Mid-Infrared Imaging of Phase Separation in a Drug–Polymer Blend," *2066 J. Pharm. Sci.*, vol. 101, no. 6, pp. 2067–2073, 2012.

[118] M. Christensen, J. T. Rasmussen, and A. C. Simonsen, "Roughness analysis of single nanoparticles applied to atomic force microscopy images of hydrated casein micelles," *Food Hydrocoll.*, vol. 45, pp. 168–174, 2015.

[119] J. G. Rosas and M. Blanco, "A criterion for assessing homogeneity distribution in hyperspectral images. Part 2: Application of homogeneity indices to solid pharmaceutical dosage forms," *J. Pharm. Biomed. Anal.*, vol. 70, pp. 691–699, 2012.

[120] K. . Cramer, J. A., & Booksh, *Chaos theory in chemistry and chemometrics: a review.* J.Chemometrics, 2006.

[121] R. Lopes and N. Betrouni, "Fractal and multifractal analysis: A review," *Med. Image Anal.*, vol. 13, no. 4, pp. 634–649, 2009.

[122] Shin Etsu, "Hypromellose Acetate Succinate NF Technical Information," *Usp Nf,* pp. 1–20, 2005.

[123] K. Ueda, K. Higashi, K. Yamamoto, and K. Moribe, "The effect of HPMCAS functional groups on drug crystallization from the supersaturated state and dissolution improvement," *Int. J. Pharm.*, vol. 464, no. 1–2, pp. 205–213, 2014.

[124] M. Otsuka, Y. Maeno, T. Fukami, M. Inoue, T. Tagami, and T. Ozeki, "Solid dispersions of efonidipine hydrochloride ethanolate with improved physicochemical and pharmacokinetic properties prepared with microwave treatment," *Eur. J. Pharm. Biopharm.*, vol. 108, pp. 25–31, 2016.

[125] Q. Cheng, "Multifractality and spatial statistics," *Comput. Geosci.*, vol. 25, no. 9, pp. 949–961, 1999.

[126] J. M. Angulo and F. J. Esquivel, "Multifractal dimensional dependence assessment based on tsallis mutual information," *Entropy*, vol. 17, no. 8, pp. 5382–5401, 2015.

[127] F. Mendoza, P. Verboven, Q. T. Ho, G. Kerckhofs, M. Wevers, and B. Nicolaï, "Multifractal properties of pore-size distribution in apple tissue using X-ray imaging," *J. Food Eng.*, vol. 99, no. 2, pp. 206–215, 2010.

[128] D. E. Newbury and N. W. M. Ritchie, "Elemental mapping of microstructures by scanning electron microscopy-energy dispersive X-ray spectrometry (SEM-EDS): Extraordinary advances with the silicon drift detector (SDD)," *J. Anal. At. Spectrom.*, vol. 28, no. 7, pp. 973–988, 2013.

[129] K. Vithani *et al.*, "Sustained release solid lipid matrices processed by hot-melt extrusion (HME)," *Colloids Surfaces B Biointerfaces*, vol. 110, pp. 403–410, 2013.

[130] E. J. Y. Ling, P. Servio, and A. M. Kietzig, "Fractal and Lacunarity Analyses:

Quantitative Characterization of Hierarchical Surface Topographies," *Microsc. Microanal.*, vol. 22, no. 1, pp. 168–177, 2016.

[131] K. Edueng, D. Mahlin, and C. A. S. Bergström, "The Need for Restructuring the Disordered Science of Amorphous Drug Formulations," *Pharm. Res.*, vol. 34, no. 9, pp. 1754–1772, 2017.

[132] D. Ouyang, "Investigating the molecular structures of solid dispersions by the simulated annealing method," *Chem. Phys. Lett.*, vol. 554, pp. 177–184, 2012.

[133] D. J. Van Drooge, K. Braeckmans, W. L. J. Hinrichs, K. Remaut, S. C. De Smedt, and H. W. Frijlink, "Characterization of the mode of incorporation of lipophilic compounds in solid dispersions at the nanoscale using Fluorescence Resonance Energy Transfer (FRET)," *Macromol. Rapid Commun.*, vol. 27, no. 14, pp. 1149–1155, 2006.

[134] J. G. Rosas, S. Armenta, J. Cruz, and M. Blanco, "A new approach to determine the homogeneity in hyperspectral imaging considering the particle size," *Anal. Chim. Acta*, vol. 787, pp. 173–180, 2013.

[135] J. B. Nanubolu and J. C. Burley, "Investigating the recrystallisation behaviour of amorphous paracetamol by variable temperature Raman studies and surface Raman mapping .," *Mol. Pharm.*, vol. 9, pp. 1544–1558, 2012.

[136] M. Milne, W. Liebenberg, and M. Aucamp, "The Stabilization of Amorphous Zopiclone in an Amorphous Solid Dispersion," *AAPS PharmSciTech*, vol. 16, no. 5, pp. 1190–1202, 2015.

[137] Z. Yang, K. Nollenberger, J. Albers, J. Moffat, D. Craig, and S. Qi, "The effect of processing on the surface physical stability of amorphous solid dispersions," *Eur. J. Pharm. Biopharm.*, vol. 88, no. 3, pp. 897–908, 2014.

[138] N. K. Thakral, S. Mohapatra, G. A. Stephenson, and R. Suryanarayanan, "Compression-Induced Crystallization of Amorphous Indomethacin in Tablets: Characterization of Spatial Heterogeneity by Two- Dimensional X - ray Di ff ractometry," *Mol. Pharm.*, vol. 12, pp. 253–263, 2015.

[139] Ž. Mitić *et al.*, "Instrumental methods and techniques for structural and physicochemical characterization of biomaterials and bone tissue: A review," *Mater. Sci. Eng. C*, vol. 79, pp. 930–949, 2017.

[140] Y. Chen, J. Wang, and J. Feng, "Understanding the fractal dimensions of urban forms

through spatial entropy," *Entropy*, vol. 19, no. 11, pp. 1–18, 2017.

[141] K. Izawa, N. Hattori, and H. Okabayashi, "Growth process for fractal polymer aggregates formed by perfluorooctyltrimethoxysilane . Time-resolved small-angle X-ray scattering study," *Colloid Polym. Sci.*, vol. 278, pp. 293–300, 2000.

[142] J. Ofner *et al.*, "Image-Based Chemical Structure Determination," *Sci. Rep.*, vol. 7, no. 1, pp. 1–11, 2017.

[143] Y. Chen, "Data fusion for accurate microscopic rough surface metrology," *Ultramicroscopy*, vol. 165, pp. 15–25, 2016.

[144] H. X. Guo, J. Heinämäki, and J. Yliruusi, "Characterization of particle deformation during compression measured by confocal laser scanning microscopy," *Int. J. Pharm.*, vol. 186, no. 2, pp. 99–108, 1999.

[145] M. E. Lauer, M. Siam, J. Tardio, S. Page, J. H. Kindt, and O. Grassmann, "Rapid Assessment of Homogeneity and Stability of Amorphous Solid Dispersions by Atomic Force Microscopy—From Bench to Batch," *Pharm. Res.*, vol. 30, no. 8, pp. 2010–2022, 2013.

List of abbreviations

AFM - atomic force microscopy

AML - amlodipine

AML10 (Amlodipine 10% w/w), FEL10, GLY10, and IND10

ANOVA - analysis of variance

API - active pharmaceutical ingredient

ASD- Amorphous solid dispersions

Cl – chloride

DoE - design of experiment

dpi – dots per inch

DSC - differential scanning calorimetry

EDS - energy dispersive X-ray spectroscopy

FDA - Food and Drug Administration

 FEL - felodipine

FRET - fluorescence resonance energy transfer

GLY - glybenclamide

HME - hot-melt extrusion

HPMC-AS - hydroxypropyl methylcellulose acetate succinate

HSD - honestly significance difference

ICH - International Conference on Harmonization

IND - indomethacine

log P - partition coefficient

LSD - least significant difference

LSM - laser scanning confocal microscopy

MD - molecular dynamics simulations

MW - microwave irradiation

NIR - near infrared

pKa - dissociation constant

QbD - Quality by Design

SD - solid dispersions

SEM - scanning electron microscopy

TEM - transmission electron microscopy

U - urea

XRPD - X-ray powder diffractograms

List of symbols

1D – one dimensional

2D – two dimensional

3D – three dimensional

D_0 - capacity dimension

D_1 - information dimension

D_2 - correlation dimension

Df - fractal dimensional

Dq - moments of the distribution

$f(\alpha)$ - Hausdorff fractal dimension

i^{th} - box density

$N(\varepsilon)$ - number of boxes

pc - percolation threshold

P_i - probability

q - moment order

Tg - glass transition temperature (Tg)

wt% - weight percentage

X (q, ε) - partition function

α_i - singularity strength

ε - grid size

List of figures

List of tables